Inorg. Chem. **2006**, *45*, 8342–8354

Syntheses, Characterization, and Catalytic Ability in Alkane Oxygenation of Chloro(dimethyl sulfoxide)ruthenium(II) Complexes with Tris(2-pyridylmethyl)amine and Its Derivatives[1,2]

Motowo Yamaguchi,* Hiroyuki Kousaka, Shinichi Izawa, Yoshiki Ichii, Takashi Kumano, Dai Masui, and Takamichi Yamagishi

Department of Applied Chemistry, Graduate School of Engineering, Tokyo Metropolitan University, Minami-osawa, Hachioji, Tokyo 192-0397, Japan

Received April 28, 2006

New ruthenium(II) complexes having a tetradentate ligand such as tris(2-pyridylmethyl)amine (TPA), tris[2-(5-methoxycarbonyl)pyridylmethyl]amine [5-$(MeOCO)_3$-TPA], tris(2-quinolylmethyl)amine (TQA), or bis(2-pyridylmethyl)-glycinate (BPG) have been prepared. The reaction of the ligand with $[RuCl_2(Me_2SO)_4]$ resulted in a mixture of trans and cis isomers of the chloro(dimethyl sulfoxide-κS)ruthenium(II) complexes containing a TPA or a BPG, whereas a trans(Cl,N_{amino}) isomer was selectively obtained for 5-$(MeOCO)_3$-TPA and TQA. The trans and cis isomers of the $[RuCl(TPA)(Me_2SO)]^+$ complex were easily separated by fractional recrystallization. The molecular structures of *trans*- and *cis*(Cl,N_{amino})-$[RuCl(TPA)(Me_2SO)]^+$ complexes and the *trans*(Cl,N_{amino})-$[RuCl\{5\text{-}(MeOCO)_3\text{-}TPA\}(Me_2SO)]^+$ complex have been determined by X-ray structural analyses. The reaction of TPA with $[RuCl_2(PhCN)_4]$ gave a single isomer of the chloro(benzonitrile)ruthenium(II) complex, whereas the bis(benzonitrile)ruthenium(II) complex was obtained with BPG. The *cis*(Cl,N_{amino})-$[RuCl(TPA)(Me_2SO)]^+$ complex is thermodynamically much less stable than the trans isomer and isomerizes in dimethyl sulfoxide at 65–100 °C. Oxygenation of alkanes catalyzed by these ruthenium(II) complexes has been examined. The chloro(dimethyl sulfoxide-κS)ruthenium(II) complexes with TPA and its derivatives using *m*-chloroperbenzoic acid as a cooxidant showed high catalytic ability. Adamantane was efficiently and selectively oxidized to give 1-adamantanol up to 88%. The chloro(dimethyl sulfoxide-κS)-ruthenium(II) complex with 5-$(MeOCO)_3$-TPA was found to be the most active catalyst among the complexes examined.

Introduction

Tripodal tetradentate ligands, TPA and its derivatives, containing both σ-donating tertiary amine and π-accepting pyridyl groups are versatile ligands and have been used for the preparation of various transition-metal complexes containing the group 5−11 elements, lanthanides, and an actinide.[3] These ligands have been employed in the structural and/or functional model complexes of mono- and dinuclear metalloenzymes[4] containing Fe[5,6] or Cu[7,8] sites as dioxygen activation centers. Ru analogues have been also studied.

The development of an efficient catalyst capable of oxidizing saturated hydrocarbons under mild conditions is a

* To whom correspondence should be addressed. E-mail: yamaguchi-motowo@c.metro-u.ac.jp. Fax: +81-426-77-1223.

(1) Preliminary communication: Yamaguchi, M.; Kousaka, H.; Yamagishi, T. *Chem. Lett*. **1997**, 769−770.

(2) Abbreviations: TPA = tris(2-pyridylmethyl)amine; 5-$(MeOCO)_3$-TPA = tris[2-(5-methoxycarbonyl)pyridylmethyl]amine; TQA = tris(2-quinolylmethyl)amine; BPGH = bis(2-pyridylmethyl)glycine.

(3) The survey of the Cambridge Crystallographic Data Centre revealed that the crystal structures of the transition-metal complexes of TPA and derivatives of V, Cr, Mn, Re, Fe, Ru, Os, Co, Rh, Ir, Ni, Cu, Nd, Eu, Tb, Lu, and U have been reported.

(4) (a) Funabiki, T. *Oxygenases and Model Systems*; Kluwer Academic Publishers: Dordrecht, The Netherlands, 1997; Chapter 3. (b) Ito, M.; Fujisawa, K.; Kitajima, N.; Moro-oka, Y. *Oxygenases and Model Systems*; Kluwer Academic Publishers: Dordrecht, The Netherlands, 1997; Chapter 8.

(5) Mononuclear models: (a) Funabiki, T.; Yamazaki, T.; Fukui, A.; Tanaka, T.; Yoshida, S. *Angew. Chem., Int. Ed*. **1998**, *37*, 513−515. (b) Costas, M.; Mehn, M. P.; Jensen, M. P.; Que, L., Jr. *Chem. Rev*. **2004**, *104*, 939−986.

(6) Dinuclear models: (a) Tshuva, Y.; Lippard, S. J. *Chem. Rev*. **2004**, *104*, 987−1012. (b) Wasser, I. M.; Huang, H.-W.; Moënne-Loccoz, P.; Karlin, K. D. *J. Am. Chem. Soc*. **2005**, *127*, 3310−3320.

(7) Cu−Fe models: (a) Kim, E.; Chufan, E. E.; Kamaraj, K.; Karlin, K. D. *Chem. Rev*. **2004**, *104*, 1077−1133. (b) Chishiro, T.; Shimazaki, Y.; Tani, F.; Naruta, Y. *Chem. Commun*. **2005**, 1079−1081.

(8) Cu−Cu models: Yamaguchi, S.; Wada, A.; Funahashi, Y.; Nagatomo, S.; Kitagawa, T.; Jitsukawa, K.; Masuda, H. *Eur. J. Inorg. Chem*. **2003**, *24*, 4378−4386.

10.1021/ic060722c CCC: $33.50
Published on Web 09/06/2006

challenging goal in synthetic chemistry, and the transition-metal complexes are promising candidates as an alkane oxidation catalyst.[9] A number of mono- and dinuclear iron complexes have been studied as a functional model of non-heme iron enzymes such as methane monooxygenase (MMO).[4b,5,10] Ruthenium complexes have drawn much attention as a functional model of MMO and have shown high catalytic ability upon alkane oxygenation.[1,11,12]

A number of the iron mononuclear complexes with TPA or BPG and their derivatives have been examined in the catalytic oxygenation of alkanes.[5,13] On the other hand, similar studies utilizing Ru-TPA complexes are few. Kojima et al. have reported alkane oxygenation catalyzed by mono- and dinuclear ruthenium complexes having TPA, $[RuCl_2(TPA)]ClO_4$, or $[RuCl(TPA)]_2(ClO_4)_2$ in the presence of *m*-chloroperbenzoic acid (MCPBA),[11a] *tert*-butyl hydroperoxide,[11c] or molecular oxygen.[11b] We have reported the preparation of the chloro(dimethyl sulfoxide-*κS*) complex with TPA[14] and its application to catalytic oxygenation of alkane.[1] It was found that *trans*(Cl,N_{amino})-[RuCl(TPA)-(Me_2SO)]PF_6 showed high catalytic ability upon oxygenation of adamantane to give 1-adamantanol selectively in high yield in the presence of MCPBA. Recently, Jituskawa et al. have reported alkane oxygenation in the presence of PhIO catalyzed by monochloro- or dichlororuthenium complexes with a TPA-type ligand having a 6-neopentylamino or 6-pivalamide group on the pyridyl group(s).[11d,e] The substituents at the 6 position of the TPA-type ligand may have both a steric effect and an electronic effect on the catalytic ability.

In this paper, we report the syntheses, characterization, and application to catalytic alkane oxygenation of the ruthenium complexes with a tripodal tetradentate ligand: TPA, 5-$(MeOCO)_3$-TPA, TQA, and BPG. The molecular structures of *trans*(Cl,N_{amino})-[RuCl(TPA)(Me_2SO)][$RuCl_3(Me_2SO)_3$],[15] *cis*(Cl,N_{amino})-[RuCl(TPA)(Me_2SO)]PF_6·$^1/_2$MeCN,[1] and *trans*-(Cl,N_{amino})-[RuCl{5-$(MeOCO)_3$-TPA}(Me_2SO)]PF_6·$0.2H_2O$[16] complexes have been determined. The bulky 6-position substituents may hinder access of the substrate and/or oxidant to the metal center, while the 5-position substituent has little steric hindrance and is expected to show only an electronic effect. We have prepared both trans and cis isomers of [RuCl(TPA)(Me_2SO)]X (X = Cl, PF_6);[1] however, Kojima et al. reported the synthesis of *cis*(Cl,N_{amino})-[RuCl(TPA)(Me_2SO)]ClO_4,[14] and Bjernemose et al. recently reported the selective synthesis of *trans*(Cl,N_{amino})-[RuCl-(TPA)(Me_2SO)]PF_6.[17] The inconsistency in the selectivity on the syntheses prompted us to study the stability of these isomers by thermal isomerization experiments, molecular mechanics (MM), and quantum mechanics (QM) calculations to shed light on the character of chloro(dimethyl sulfoxide-*κS*)ruthenium(II) complexes with TPA and its derivatives. The results of the oxygenation of alkanes catalyzed by these ruthenium(II) complexes are also reported. The study of complexes involving a TPA with electron-withdrawing groups has thus far been rare, and the ruthenium(II) complex [RuCl{5-$(MeOCO)_3$-TPA}(Me_2SO)]PF_6 having methoxycarbonyl group on the pyridyl groups was found to be an active and selective catalyst on the oxygenation of alkanes.

Experimental Section

Materials and Measurements. All chemicals were of reagent grade and were used as received without further purification unless otherwise noted. TPA,[18] TQA,[19] BPGH,[18] *cis*-[$RuCl_2(Me_2SO)_4$],[20] and *trans*-[$RuCl_2(PhCN)_4$][21] were prepared by literature procedures. The solvents used for catalytic oxidation reaction were purified by refluxing over P_2O_5 or $KMnO_4$ (for acetone), distilled, and stored in a N_2 atmosphere.

NMR spectra were recorded on JEOL EX-270 or JEOL LA-400 spectrometers. Fast atom bombardment mass spectra (FAB-MS) were obtained on a JEOL LX-1000 mass spectrometer by using *m*-nitrobenzyl alcohol as a matrix. The isotopic distributions of Ru complex ions were calculated to assign the observed peaks.

All electrochemical measurements were carried out with a BAS CV50W voltammetry analyzer in acetonitrile using 0.1 M tetraethylammonium perchlorate as the supporting electrolyte under N_2 at ambient temperature. Cyclic voltammograms (CV) were obtained

(9) (a) Hill, C. R., Ed. *Activation and Functionalization of Alkanes*; Wiley-Interscience: New York, 1989. (b) Shilov, A. E.; Shul'pin, G. B. *Activation and Catalytic Reactions of Saturated Hydrocarbons in the Presence of Metal Complexes*; Kluwer Academic Publishers: Dordrecht, The Netherlands, 2000.

(10) Hu, Z.; Gorun, S. M. *Biomimetic Oxidations Catalyzed by Transition Metal Complexes*; Imperial College Press: London, 2000; Chapter 6.

(11) Ruthenium catalysts containing TPA or its derivatives: (a) Kojima, T. *Chem. Lett.* **1996**, 121−122. (b) Kojima, T.; Matsuda, Y. *Chem. Lett*. **1999**, 81−82. (c) Kojima, T.; Matsuo, H.; Matsuda, Y. *Inorg. Chim. Acta* **2000**, *300*−*302*, 661−667. (d) Jitsukawa, K.; Oka, Y.; Einaga, H.; Masuda, H. *Tetrahedron Lett*. **2001**, *42*, 3467−3469. (e) Jitsukawa, K.; Oka, Y.; Yamaguchi, S.; Masuda, H. *Inorg. Chem.* **2004**, *43*, 8119−8129.

(12) Ruthenium catalysts containing a ligand(s) other than TPA: (a) Che, C.-M. *Pure Appl. Chem.* **1995**, *67*, 225−232. (b) Meyer, T. J.; Huynh, M. H. V. *Inorg. Chem.* **2003**, *42*, 8140−8160. (c) Taqui Khan, M. M.; Chatterjee, D.; Merchant, R. R.; Paul, P.; Abdi, S. H. R.; Srinivas, D.; Siddiqui, M. R. H.; Moiz, M. A.; Bhadbhade, M. M.; Venkatasubramanian, K. *Inorg. Chem.* **1992**, *31*, 2711−2718. (d) Naota, T.; Takaya, H.; Murahashi, S.-I. *Chem. Rev.* **1998**, *98*, 2599−2660. (e) Goldstein, A. S.; Beer, R. H.; Drago, R. S. *J. Am. Chem. Soc*. **1994**, *116*, 2424−2429. (f) Yamaguchi, M.; Iida, T.; Yamagishi, T. *Inorg. Chem. Commun.* **1998**, 299−301. (g) Yamaguchi, M.; Ichii, Y.; Kosaka, S.; Masui, D.; Yamagishi, T. *Chem. Lett*. **2002**, 434−435.

(13) (a) Leising, R. A.; Norman, R. E.; Que, L., Jr. *Inorg. Chem*. **1990**, *29*, 2553−2555. (b) Leising, R. A.; Kim, J.; Pèrez, M. A.; Que, L., Jr. *J. Am. Chem. Soc*. **1993**, *115*, 9524−9530. (c) Kim, J.; Harrison, R. G.; Kim, C.; Que, L., Jr. *J. Am. Chem. Soc*. **1996**, *118*, 4373−4379. (d) Chen, K.; Que, L., Jr. *J. Am. Chem. Soc*. **2001**, *123*, 6327−6337. (e) Rohde, J.-U.; Torelli, S.; Shan, X.; Lim, M. H.; Klinker, E. J.; Kaizer, J.; Chen, K.; Nam, W.; Que, L., Jr. *J. Am. Chem. Soc*. **2004**, *126*, 16750−16761.

(14) After our publication in ref 1, the study of *cis*(Cl,N_{amino})-[RuCl(TPA)-(Me_2SO)]ClO_4 and *trans*(Cl,N_{amino})-[RuCl(5-Me_3-TPA)(Me_2SO)]ClO_4 has been reported by Kojima and colleagues: Kojima, T.; Amano, T.; Ishii, Y.; Ohba, M.; Okaue, Y.; Matsuda, Y. *Inorg. Chem.* **1998**, *37*, 4076−4085.

(15) Masui, D.; Yamaguchi, M.; Yamagishi, T. *Acta Crystallogr. E* **2003**, *E59*, m308−309.

(16) Yamaguchi, M.; Kumano, T.; Masui, D.; Yamagishi, T. *Chem. Commun*. **2004**, 798−799.

(17) Bjernemose, J.; Hazell, A.; McKenzie, C. J.; Mahon, M. F.; Nielsen, L. P.; Raithby, P. R.; Simonsen, O.; Toftlund, H.; Wolny, J. A. *Polyhedron* **2003**, *22*, 875−885.

(18) Cox, D. D.; Benkovic, S. J.; Bloom, L. M.; Bradley, F. C.; Nelson, M. J.; Que, L., Jr.; Wallick, D. E. *J. Am. Chem. Soc*. **1988**, *110*, 2026−2032.

(19) Wei, N.; Murthy, N. N.; Chen, Q.; Zubieta, J.; Karlin, K. D. *Inorg. Chem*. **1994**, *33*, 1953−1965.

(20) Evans, I. E.; Spencer, A.; Wilkinson, G. *J. Chem. Soc., Dalton Trans*. **1973**, 204−209.

(21) Johnson, B. F. G.; Lewis, J.; Ryder, I. E. *J. Chem. Soc., Dalton Trans*. **1977**, 719−724.

by using a platinum disk (3-mm-o.d.) working electrode, a platinum wire counter electrode, and an Ag/Ag^+ reference electrode. Redox potentials were determined relative to a ferrocene/ferrocenium (Fc/Fc^+) ion couple as 0 V. All solutions were deoxygenated by bubbling N_2 gas through them and were maintained under N_2 during the measurements. Analyses of the oxygenated products were performed by a Shimadzu GC-14a gas chromatograph using the G100 column of the Chemicals Evaluation and Research Institute, Japan (Tokyo, Japan), or a Shimadzu GCMS-QP5050 gas chromatograph/mass spectrometer.

MM calculations were performed using Fujitsu CAChe version 4.4 on a PC Celeron platform. Density functional theory (DFT) calculations were performed using the *Gaussian98* package[22] for UNIX, on the IBM parallel computer p690-681 located in the Computing Center at Tokyo Metropolitan University. The basis set LANL2DZ or 3-21G** was applied for B3LYP calculations.

Methyl 6-(Bromomethyl)nicotinate. Methyl 6-(bromomethyl)-nicotinate was prepared by bromination of methyl 6-methylnicotinate using *N*-bromosuccinimide/benzoyl peroxide[23] or methyl 6-(hydroxymethyl)nicotinate[24] using CBr_4/PPh_3. The latter procedure resulted in better yield as follows.

Methyl 6-(hydroxymethyl)nicotinate (3.21 g, 19.2 mmol) and tetrabromomethane (8.04 g, 24.3 mmol) were dissolved in a minimal amount of tetrahydrofuran (THF). The resultant solution was stirred for 2 h at room temperature. To the solution was added water, and the reaction mixture was extracted by dichloromethane three times, dried by magnesium sulfate, filtered, and concentrated by evaporation. The residue was purified by column chromatography (SiO_2; hexane:ethyl acetate = 3:2). A reddish solid was obtained after evaporation of the solvent. Yield: 2.85 g (64%). FAB-MS: $(M + H)^+$ 230, 232. ^{1}H NMR ($CDCl_3$, 270 MHz): δ 3.94 (3H, s, Me), 4.56 (2H, s, C*H*$_2$), 7.52 (1H, d, $J = 7.8$ Hz, py-H3), 8.28 (1H, dd, $J = 7.8$ Hz, 2.0 Hz, py-H4), 9.14 (1H, d, $J = 2.0$ Hz, py-H6).

Tris[2-(5-methoxycarbonyl)pyridylmethyl]amine [5-$(MeOCO)_3$-TPA]. 5-$(MeOCO)_3$-TPA was prepared from methyl 6-(bromomethyl)nicotinate by a slightly modified method for the preparation of TQA.[19] To a solution of methyl 6-(bromomethyl)nicotinate (2.756 g, 12 mmol) in 15 mL of THF was added 1.24 mL (16 mmol) of aqueous ammonium hydroxide in four equal portions. The reaction mixture turned instantly red with the addition of aqueous ammonium hydroxide. The solution was stirred at room temperature, and the following portions of aqueous ammonium hydroxide were added after the color disappeared (it took about 24 h). The reaction mixture was stirred for 1 week. The colorless solid was filtered, and the filtrate was concentrated to dryness. The residue was dissolved in methylene chloride and dried with magnesium sulfate. After filtration, the filtrate was evaporated to dryness to yield a slightly yellowish solid. Yield: 1.45 g (78%). FAB-MS: $(M + 1)^+$ 465. ^{1}H NMR ($CDCl_3$, 270 MHz): δ 3.94 (9H, s, Me), 3.97 (6H, s, C*H*$_2$), 7.63 (3H, d, $J = 7.9$ Hz, py-H3), 8.26 (3H, dd, $J = 7.9$ Hz, 2.0 Hz, py-H4), 9.14 (3H, d, $J = 2.0$ Hz, py-H6).

[RuCl(TPA)(Me_2*S*O)]Cl (1). A solution of TPA (0.41 g, 1.4 mmol) and *cis*-$[RuCl_2(Me_2SO)_4]$ (0.68 g, 1.4 mmol) in 80 mL of methanol was refluxed for 2 h. The reaction mixture was concentrated to dryness, and the resulting solid was dissolved in a small amount of methanol. After the addition of ethyl acetate, the solution was kept in a refrigerator overnight. Yellow precipitates were collected and dried in vacuo. Yield: 0.70 g (92%). FAB-MS: $(M - Cl)^+$ 505.

***cis*(Cl,N_{amino})-[RuCl(TPA)(Me_2*S*O)]Cl (2) and *trans*(Cl,N_{amino})-[RuCl(TPA)(Me_2*S*O)]Cl (3).** The above complex **1** was a mixture of an approximately equal amount of the trans and cis isomers, which was isolated by careful fractional recrystallizations from methanol and ethyl acetate (1:10, v/v). The cis isomer (**2**) and the trans isomer (**3**) were obtained as yellow and pale-orange powders, respectively. The complex **2** was less soluble. Yield: 0.24 g (32%) for **2** and 0.35 g (47%) for **3**. FAB-MS: $(M - Cl)^+$ 505 for **2** and **3**. ^{1}H NMR (CD_3CN, 270 MHz) for **2**: δ 3.42 (6H, s, C*H*$_3$), 4.69 (2H, s, C*H*$_2$(ax)), 4.79 (2H, d, $J = 15$ Hz, C*H*$_2$(eq)), 5.76 (2H, d, $J = 15$, C*H*$_2$(eq)), 6.95 (1H, d, $J = 7.9$ Hz, py-H3(ax)), 7.16−7.25 (3H, m, py-H5(ax + eq)), 7.46−7.51 (3H, m, py-H4(ax) + py-H3(eq)), 7.73 (2H, t, $J = 7.8$ Hz, py-H4(eq)), 8.70 (2H, d, $J = 5.6$ Hz, py-H6(eq)), 9.81 (1H, d, $J = 5.6$ Hz, py-H6(ax)). ^{1}H NMR for **3**: 2.84 (6H, s, C*H*$_3$), 4.53 (2H, s, C*H*$_2$(ax)), 4.72 (2H, d, $J = 15$ Hz, C*H*$_2$(eq)), 5.39 (2H, d, $J = 15$ Hz, C*H*$_2$(ax)), 7.13 (1H, d, $J = 7.9$ Hz, py-H3(ax)), 7.26−7.36 (3H, m, py-H5(ax + eq)), 7.43 (2H, d, $J = 7.9$ Hz, py-H3(eq)), 7.64 (1H, t, $J = 7.9$ Hz, py-H4(ax)), 7.76 (2H, t, $J = 7.8$ Hz, py-H4(eq)), 8.75 (2H, d, $J = 5.3$ Hz, py-H6(eq)), 9.69 (1H, d, $J = 5.6$ Hz, py-H6(ax)).

***trans*(Cl,N_{amino})-[RuCl(TPA)(Me_2*S*O)][$RuCl_3(Me_2SO)_3$] (4).** The trans(Cl,N_{amino}) isomer was obtained unintentionally as the salt with a $[RuCl_3(Me_2SO)_3]$ anion from the reaction mixture of the complex **1**. See text.

***cis*(Cl,N_{amino})-[RuCl(TPA)(Me_2*S*O)]PF_6·½MeCN (5·½MeCN).** The crude chloride salt, complex **1** (0.32 g, 0.59 mmol), and NH_4PF_6 (0.099 g, 0.61 mmol) were dissolved in 15 mL of methanol, and the solution was evaporated to dryness. The solid was dissolved in 20 mL of acetonitrile and filtered. The filtrate was evaporated to dryness. The resulting yellow powder was dried in vacuo. The hexafluorophosphate salt, which was a mixture of the trans and cis isomers, was dissolved in 2 mL of acetonitrile. To the resultant solution was slowly added 3 mL of diethyl ether, and the solution was kept in a refrigerator overnight. Orange crystals were collected and dried in vacuo. This procedure was repeated three times and gave 0.182 g (47%) of a single isomer, which was found to be the cis(Cl,N_{amino}) isomer by X-ray analysis. See below. Anal. Calcd for $C_{21}H_{25.5}ClF_6N_{4.5}OPRuS$: C, 37.62; H, 3.83; N, 9.40. Found: C, 37.57; H, 3.86; N, 9.28. FAB-MS: $(M - PF_6)^+$ 505. ^{1}H NMR (CD_3CN, 270 MHz): δ 3.43 (6H, s, C*H*$_3$), 4.67 (2H, s, C*H*$_2$(ax)), 4.77 (2H, d, $J = 15$ Hz, C*H*$_2$(eq)), 5.77 (2H, d, $J = 15$ Hz, C*H*$_2$(eq)), 6.95 (1H, d, $J = 7.9$ Hz, py-H3(ax)), 7.16−7.26 (3H, m, py-H5(ax + eq)), 7.46−7.52 (3H, m, py-H4(ax) + py-H3(eq)), 7.74 (2H, t, $J = 7.8$ Hz, py-H4(eq)), 8.70 (2H, d, $J = 5.6$ Hz, py-H6(eq)), 9.81 (1H, d, $J = 5.6$ Hz, py-H6(ax)). A peak assigned to acetonitrile was observed at 2.00 ppm in $CDCl_3$.

***trans*(Cl,N_{amino})-[RuCl(TPA)(Me_2*S*O)]PF_6 (6).** The grayish-orange crystals, which were the trans(Cl,N_{amino}) isomer, were obtained from the filtrate of the above-mentioned fractional recrystallization. Yield: 0.111 g (29%). Anal. Calcd for $C_{20}H_{24}ClF_6N_4OPRuS$: C, 37.13; H, 3.74; N, 8.65. Found: C, 37.13; H, 3.74; N, 8.65. FAB-MS: $(M - PF_6)^+$ 505. ^{1}H NMR (CD_3CN, 270

(22) Frisch, M. J.; Trucks, G. W.; Schlegel, H. B.; Scuseria, G. E.; Robb, M. A.; Cheeseman, J. R.; Zakrzewski, V. G.; Montgomery, J. A., Jr.; Stratmann, R. E.; Burant, J. C.; Dapprich, S.; Millam, J. M.; Daniels, A. D.; Kudin, K. N.; Strain, M. C.; Farkas, O.; Tomasi, J.; Barone, V.; Cossi, M.; Cammi, R.; Mennucci, B.; Pomelli, C.; Adamo, C.; Clifford, S.; Ochterski, J.; Petersson, G. A.; Ayala, P. Y.; Cui, Q.; Morokuma, K.; Salvador, P.; Dannenberg, J. J.; Malick, D. K.; Rabuck, A. D.; Raghavachari, K.; Foresman, J. B.; Cioslowski, J.; Ortiz, J. V.; Baboul, A. G.; Stefanov, B. B.; Liu, G.; Liashenko, A.; Piskorz, P.; Komaromi, I.; Gomperts, R.; Martin, R. L.; Fox, D. J.; Keith, T.; Al-Laham, M. A.; Peng, C. Y.; Nanayakkara, A.; Challacombe, M.; Gill, P. M. W.; Johnson, B.; Chen, W.; Wong, M. W.; Andres, J. L.; Gonzalez, C.; Head-Gordon, M.; Replogle, E. S.; Pople, J. A. *Gaussian 98*, revision A.11; Gaussian, Inc.: Pittsburgh, PA, 2001.
(23) Tyeklar, Z.; Jacobson, R. R.; Wei, N.; Murthy, N. N.; Zubieta, J.; Karlin, K. D. *J. Am. Chem. Soc*. **1993**, *115*, 2677−2689.
(24) Tachi, Y.; Aita, K.; Teramae, S.; Tani, F.; Naruta, Y.; Fukuzumi, S.; Itoh, S. *Inorg. Chem*. **2004**, *43*, 4558−4560.

MHz): δ 2.85 (6H, s, CH_3), 4.49 (2H, s, CH_2(ax)), 4.67 (2H, d, J = 15 Hz, CH_2(eq)), 5.41 (2H, d, J = 15 Hz, CH_2(ax)), 7.12 (1H, d, J = 7.9 Hz, py-H3(ax)), 7.27−7.32 (3H, m, py-H5(ax + eq)), 7.43 (2H, d, J = 7.9 Hz, py-H3(eq)), 7.63 (1H, t, J = 7.9 Hz, py-H4(ax)), 7.77 (2H, t, J = 7.8 Hz, py-H4(eq)), 8.76 (2H, d, J = 5.3 Hz, py-H6(eq)), 9.70 (1H, d, J = 5.6 Hz, py-H6(ax)).

***trans*(Cl,N_{amino})-[RuCl{5-$(MeOCO)_3$-TPA}(Me_2SO)]Cl (7).** The complex **7** was obtained in a procedure similar to that of complex **1** using 5-$(MeOCO)_3$-TPA and *cis*-[$RuCl_2(Me_2SO)_4$] except that the resulting product was recrystallized from methanol/ethyl acetate and the orange crystals obtained were the trans(Cl,N_{amino}) isomer. Yield: 88%. FAB-MS: $(M - Cl)^+$ 679, $(M - Cl - Me_2SO)^+$ 601. ^{1}H NMR ($CDCl_3$, 270 MHz): δ 2.93 (6H, s, Me_2SO), 3.95 (6H, s, CH_3OCO), 3.98 (3H, s, CH_3OCO), 5.38 (2H, s, CH_2(ax)), 5.42 (2H, d, J = 15.5 Hz, CH_2(eq)), 5.81 (2H, d, J = 15.5 Hz, CH_2(eq)), 7.64 (1H, d, J = 8.2 Hz, py-H3(ax)), 7.82 (2H, J = 8.2 Hz, py-H3(eq)), 8.17 (1H, dd, J = 2.0 and 8.2 Hz, py-H4(ax)), 8.29 (2H, dd, J = 2.0 and 8.2 Hz, py-H4(eq)), 9.33 (2H, d, J = 2.0 Hz, py-H6(eq)), 10.29 (1H, d, J = 2.0 Hz, py-H6(ax)).

***trans*(Cl,N_{amino})-[RuCl{5-$(MeOCO)_3$-TPA}(Me_2SO)]PF_6·$0.2H_2O$ (8).** Complex **7** was converted to the PF_6 salt for elemental analysis. [RuCl(Me_2SO){5-$(MeOCO)_3$-TPA}]PF_6·$0.2H_2O$. Anal. Calcd for $C_{26}H_{30.4}ClF_6N_4O_{7.2}PRuS$: C, 37.73; H, 3.70; N, 6.77. Found: C, 37.73; H, 3.46; N, 6.80. FAB-MS (*m*-NBA): $(M - PF_6)^+$ 679, $(M - PF_6 - Me_2SO)^+$ 601. ^{1}H NMR (CD_3CN, 270 MHz): δ 2.86 (6H, s, $(CH_3)_2SO$), 3.89 (6H, s, CH_3OCO), 3.93 (3H, s, CH_3OCO), 4.59 (2H, s, CH_2(ax)), 4.82 (2H, d, J = 15.5 Hz, CH_2(eq)), 5.44 (2H, d, J = 15.5 Hz, CH_2(eq)), 7.24 (1H, d, J = 8.2 Hz, py-H3(ax)), 7.57 (2H, d, J = 8.2 Hz, py-H3(eq)), 8.16 (1H, dd, J = 2.0 and 8.2 Hz, py-H4(ax)), 8.27 (2H, dd, J = 2.0 and 8.2 Hz, py-H4(eq)), 9.20 (2H, d, J = 2.0 Hz, py-H6(eq)), 10.22 (1H, d, J = 2.0 Hz, py-H6(ax)).

***trans*(Cl,N_{amino})-[RuCl(TQA)(Me_2SO)]Cl (9).** The complex **9** was obtained in a procedure similar to that of complex **1** using TQA and *cis*-[$RuCl_2(Me_2SO)_4$] except that the resulting brown powder was the trans(Cl,N_{amino}) isomer. See the text. Yield: 62%. Anal. Calcd for $C_{32}H_{30}Cl_2N_4ORuS$: C, 55.65; H, 4.38; N, 8.11. Found: C, 55.88; H, 4.62; N, 7.90. FAB-MS: $(M - Cl - Me_2SO)^+$ 577. ^{1}H NMR (($CD_3)_2SO$, 270 MHz): δ 2.93* (6H, s, CH_3), 5.06 (2H, s, CH_2(ax)), 5.23 (2H, d, J = 16.5 Hz, CH_2(eq)), 6.07 (2H, d, J = 16.5 Hz, CH_2(eq)), 7.30 (1H, d, J = 8.6 Hz, qn-H5(ax)), 7.50−7.64 (5H, m, qn-H6(ax) + qn-H6(eq) + qn-H7(eq)), 7.67 (2H, d, J = 8.4 Hz, qn-H3(eq)), 7.80 (1H, d, J = 7.6 Hz, qn-H3(ax)), 7.91 (2H, d, J = 8.7 Hz, qn-H5(eq)), 8.02 (1H, t, J = 8.0 Hz, qn-H7(ax)), 8.24 (1H, d, J = 7.6 Hz, qn-H4(ax)), 8.48 (2H, d, J = 8.4 Hz, qn-H4(eq)), 9.67 (2H, d, J = 8.6 Hz, qn-H8(eq)), 11.02 (1H, d, J = 8.0 Hz, qn-H8(ax)). An asterisk indicates that the CH_3 peak of the Me_2SO was not observed because of overlapping with the solvent peak but was observed in $CDCl_3$.

[Ru(BPG)Cl(Me_2SO)]·H_2O (10·H_2O). To 20 mL of methanol was added *cis*-[$RuCl_2(Me_2SO)_4$] (0.356 g, 0.734 mmol), and the mixture was heated at 80 °C. To the resultant mixture was added at one time a solution of BPGH (0.380 g, 1.48 mmol) and KOH (0.093 g, 1.7 mmol) in 20 mL of methanol. After refluxing for 2 h, the solution was concentrated to about 5 mL and kept in a refrigerator. The precipitates were filtered and washed with ethyl acetate. The solid was dissolved in chloroform, filtered, evaporated to dryness, and dried in vacuo. Complex **9** is a mixture of the trans and cis isomers. Yield: 0.039 g (11%). Anal. Calcd for $C_{16}H_{20}ClN_3O_3RuS$·H_2O: C, 39.30; H, 4.53; N, 8.49. Found: C, 39.36; H, 4.46; N, 8.06. FAB-MS: M^+ 471. ^{1}H NMR ($CDCl_3$, 270 MHz): δ 3.62 (6H, s, CH_3), 3.67 (6H, s, CH_3), 3.77 (2H, s, CH_2CO_2), 3.79 (2H, s, CH_2CO_2), 4.52 (2H, d, J = 14 Hz, py-CH_2(eq)), 4.58 (2H, d, J = 14 Hz, py-CH_2(eq)), 5.82 (2H, d, J = 14 Hz, py-CH_2(eq)), 5.94 (2H, d, J = 14 Hz, py-CH_2(eq)), 7.24−7.31 (8H, m, py-H3 + py-H5), 7.62 (4H, t, J = 7.3 Hz, py-H4), 9.00 (4H, d, J = 5.6 Hz, py-H6).

[RuCl(PhCN)(TPA)]Cl (11). A mixture of TPA (0.204 g, 0.70 mmol) and *trans*-[$RuCl_2(PhCN)_4$] (0.409 g, 0.70 mmol) in 50 mL of methanol was heated to reflux for 2 h. After evaporation to dryness, the resulting solid was dissolved in methanol (1 mL). To this solution was added diethyl ether (10 mL), and the resulting solution was then kept in a refrigerator for 2 weeks. The orange precipitates were collected and dried in vacuo. Complex **11** contains only one isomer. Yield: 0.071 g (18%). Anal. Calcd for $C_{25}H_{23}Cl_2N_5Ru$: C, 53.10; H, 4.10; N, 12.39. Found: C, 52.92; H, 4.01; N, 12.44. FAB-MS: $(M - Cl)^+$ 530. ^{1}H NMR (CD_3CN, 270 MHz): δ 4.64 (2H, s, CH_2(ax)), 4.78 (2H, d, J = 15 Hz, CH_2(eq)), 5.43 (2H, d, J = 15 Hz, CH_2(eq)), 7.01 (1H, d, J = 7.8 Hz, py-H3(ax)), 7.13 (1H, t, J = 7.7 Hz, py-H5(ax)), 7.26 (2H, t, J = 7.6 Hz, py-H5(eq)), 7.43 (2H, t, J = 7.9 Hz, py-H4(eq)), 7.50 (1H, t, J = 7.8 Hz, py-H4(ax)), 7.63−7.80 (5H, m, *Ph*CN), 8.08 (2H, d, J = 7.9 Hz, py-H3(eq)), 8.82 (2H, d, J = 5.5 Hz, py-H6(eq)), 9.03 (1H, d, J = 5.6 Hz, py-H6(ax)).

[Ru(BPG)($PhCN)_2$]Cl (12). To 20 mL of methanol was added *trans*-[$RuCl_2(PhCN)_4$] (0.351 g, 0.60 mmol), and the mixture was heated at 80 °C. To the resultant mixture was added at one time a solution of BPGH (0.154 g, 0.60 mmol) and KOH (0.042 g, 0.75 mmol) in 30 mL of methanol. After refluxing for 8 h, the solution was cooled to room temperature and evaporated to dryness. The solid was dissolved in methanol (1 mL). To this solution was slowly added ethyl acetate (10 mL), and the resulting solution was then kept in a refrigerator overnight. The orange needles were collected and dried in vacuo. Yield: 0.108 g (30%). Anal. Calcd for $C_{28}H_{24}ClN_5O_2Ru$: C, 56.14; H, 4.04; N, 11.69. Found: C, 56.37; H, 4.16; N, 11.56. FAB-MS: $(M - Cl)^+$ 564. ^{1}H NMR (CD_3CN, 270 MHz): δ 3.57 (2H, s, CH_2CO_2), 4.79, 4.96 (4H, AB quartet, J = 15 Hz, py-CH_2), 7.44−7.80 (12H, m, *Ph*CN + py-H5), 7.88 (2H, t, J = 7.9 Hz, py-H4), 8.05 (2H, d, J = 7.9 Hz, py-H3), 8.89 (2H, d, J = 5.6 Hz, py-H6).

X-ray Structural Analysis of 4.[15] A good single crystal of **4** was obtained as a yellow block (0.20 × 0.10 × 0.08 mm) by the slow diffusion of ethyl acetate to a solution of complex **1** in methanol. Pertinent crystallographic data and experimental conditions are summarized in Table 1. Details of data collection and refinement have been described previously.[15] Selected bond lengths and angles are listed in Table 2.

X-ray Structural Analysis of 5·½MeCN.[1] Good single crystals of **5** containing one acetonitrile molecule per two molecules of the complex were obtained from acetonitrile and toluene as a yellow needle with the dimension of 0.2 × 0.1 × 0.1 mm^3. The presence of acetonitrile was confirmed by NMR and elemental analysis. Data collection was done on a MAC Science MXC18 four-circle diffractometer using graphite-monochromated Mo Kα radiation (λ = 0.710 73 Å). Within the range θ = 3−55°, the data were collected using a scan. A total of 5012 independent reflections were obtained, and 4962 reflections with $|F_o| \geq 2\sigma(F_o)$ were used in the further calculations. The intensities were corrected for Lorentz and polarization effects and for absorption as part of the refinement model.[25] Pertinent crystallographic data and experimental conditions are summarized in Table 1. The structure was solved by direct methods using SIR97.[26] All non-H atoms were refined anisotropi-

(25) Walker, N.; Stuart, D. *Acta Crystallogr*. **1983**, *A39*, 158−166.
(26) SIR97: Altomare, A.; Cascarano, G.; Giacovazzo, C.; Guagliardi, A.; Burla, M. C.; Polidori, G.; Camalli, M. *J. Appl. Crystallogr*. **1994**, *27*, 435−436.

Table 1. Crystallographic Data for **4**, **5**, and **8**

	4	**5**	**8**
empirical formula	$C_{26}H_{42}Cl_4N_4O_4Ru_2S_4$	$C_{21}H_{25.5}ClF_6N_{4.5}OPRuS$	$C_{26}H_{30.4}ClF_6N_4O_{7.2}PRuS$
fw	946.82	670.51	827.70
cryst syst	triclinic	monoclinic	triclinic
a, Å	10.1817(18)	19.000(4)	11.5045(9)
b, Å	14.221(2)	17.974(4)	14.2950(11)
c, Å	14.664(3)	16.262(5)	11.4761(8)
α, deg	114.362(3)	90	104.455(3)
β, deg	96.804(3)	107.65(2)	106.799(3)
γ, deg	105.610(3)	90	97.201(2)
V, Å^3	1798.1(5)	5292(2)	1709.4(2)
space group	$P\bar{1}$ (No. 2)	*C*2/*c* (No. 15)	$P\bar{1}$ (No. 2)
Z	2	4	1
D_{calc}, g/cm^3	1.749	1.683	1.608
T, K	173	293	293
μ(Mo Kα), cm^{-1}	14.07	8.90	7.25
no. of reflns used	4463	4962	7668
no. of variables	405	460	506
R^a	0.027	0.031	0.037
R_w	0.065[b]	0.076[c]	0.090[d]
GOF	0.98	1.093	1.138

[a] $R = \sum||F_o| - |F_c||/\sum|F_o|$. [b] $R_w = [\sum w(F_o^2 - F_c^2)^2/\sum w(F_o^2)^2]^{1/2}$ with weight $w = 1/[\sigma^2(F_o^2) + (0.0351P)^2]$ where $P = (F_o^2 + 2F_c^2)/3$. [c] $R_w = [\sum w(|F_o| - |F_c|)^2/\sum w|F_o|^2]^{1/2}$ with weight $w = 1/[\sigma^2(F_o^2) + (0.0374P)^2 + 6.4722P]$ where $P = (F_o^2 + 2F_c^2)/3$. [d] $R_w = [\sum w(F_o^2 - F_c^2)^2/\sum w(F_o^2)^2]^{1/2}$ with weight $w = 1/[\sigma^2(F_o^2) + (0.0594P)^2 + 0.6402P]$ where $P = (F_o^2 + 2F_c^2)/3$.

Table 2. Selected Bond Lengths (Å) and Angles (deg) for **4**, **5**, and **8**

trans(Cl,N_{amino})-[RuCl(TPA)(Me_2SO)]-[$RuCl_3$(Me_2SO)$_3$] (**4**)

Ru1−Cl1	2.4321(9)	Cl1−Ru1−S1	88.87(3)
Ru1−S1	2.2385(10)	Cl1−Ru1−N4	171.41(8)
Ru1−N1	2.078(3)	S1−Ru1−N4	98.48(8)
Ru1−N2	2.106(3)	N1−Ru1−N4	80.55(10)
Ru1−N3	2.060(3)	N2−Ru1−N4	80.75(10)
Ru1−N4	2.070(3)	N3−Ru1−N4	82.90(11)
S1−O1	1.480(2)	Cl1−Ru1−S1	88.87(3)

cis(Cl,N_{amino})-[RuCl(TPA)(Me_2SO)]PF_6·$^1/_2$MeCN (**5**)

Ru1−Cl1	2.4319(9)	Cl1−Ru1−S1	85.75(3)
Ru1−S1	2.2653(8)	Cl1−Ru1−N1	90.99(7)
Ru1−N1	2.095(2)	S1−Ru1−N1	176.13(7)
Ru1−N2	2.065(2)	N1−Ru1−N2	81.91(10)
Ru1−N3	2.079(2)	N1−Ru1−N3	80.70(10)
Ru1−N4	2.091(2)	N1−Ru1−N4	79.93(10)
S1−O1	1.479(3)		

trans(Cl,N_{amino})-[RuCl{5-($MeOCO)_3$-TPA}(Me_2SO)]PF_6·0.2H_2O (**8**)

Ru1−Cl1	2.4253(6)	Cl1−Ru1−S1	88.01(2)
Ru1−S1	2.2585(6)	Cl1−Ru1−N1	172.93(5)
Ru1−N1	2.0778(19)	S1−Ru1−N1	98.62(6)
Ru1−N2	2.060(2)	N1 Ru1−N2	82.61(8)
Ru1−N3	2.1033(19)	N1−Ru1−N3	81.28(7)
Ru1−N4	2.078(2)	N1−Ru1−N4	80.29(8)
S1−O7	1.4921(19)		

cally, and all H atoms except those of the solvent molecule were located at the calculated positions. Refinements were carried out by a full-matrix least-squares method on F^2 using *SHELXL-97*.[27] Atom scattering factors were taken from the standard source.[28] The N atom of acetonitrile was found on the rotational axis. A hexafluorophosphate anion was found to be disordered. The final discrepancy factors were $R = \sum||F_o| - |F_c||/\sum|F_o| = 0.031$ and $R_w = [\sum w(F_o^2 - F_c^2)^2/\sum w(F_o^2)^2]^{1/2} = 0.076$ with weight $w = 1/[\sigma^2(F_o^2) + (0.0374P)^2 + 6.4722P]$ where $P = (F_o^2 + 2F_c^2)/3$. Selected bond lengths and angles are listed in Table 2.

X-ray Structural Analysis of 8.[16] Good crystals suitable for X-ray analysis were obtained as an orange block (0.40 × 0.60 × 0.60 mm) by the slow diffusion of ethanol to a solution of **8** in acetone. Data collection was done on a Rigaku RAXIS−RAPID Imaging Plate diffractometer using graphite-monochromated Mo Kα radiation (λ = 0.710 69 Å). A total of 7668 independent reflections were obtained, and 7093 reflections with $|F_o| \geq 2\sigma(F_o)$ were used in the further calculations. The intensities were corrected for Lorentz and polarization effects. Pertinent crystallographic data and experimental conditions are summarized in Table 1. The structure was solved by direct methods using SIR97.[26] All non-H atoms were refined anisotropically, and all H atoms were located at the calculated positions. Refinement was carried out by a full-matrix least-squares method on F^2 using *SHELXL-97*.[27] Atom scattering factors were taken from the standard source.[28] The final discrepancy factors were $R = \sum||F_o| - |F_c||/\sum|F_o| = 0.033$ and $R_w = [\sum w(|F_o| - |F_c|)^2/\sum w|F_o|^2]^{1/2} = 0.086$ with weight $w = 1/[\sigma^2(F_o^2) + (0.0614P)^2 + 0.5193P]$ where $P = (F_o^2 + 2F_c^2)/3$. Selected bond lengths and angles are listed in Table 2.

Catalytic Oxidation of Alkanes Using Ruthenium Complexes in the Presence of MCPBA. Catalytic oxidation of adamantane, cyclooctane, and ethylbenzene using ruthenium complexes was carried out in the presence of MCPBA. A typical reaction procedure of catalytic oxidation was as follows: 0.2 mmol (0.027 g) of adamantane, 0.3 mmol (0.074 g) of MCPBA, and 1 × 10^{-3} mmol of the ruthenium complex were dissolved in 5 mL of chloroform containing 1,2-dichlorobenzene as an internal reference under a N_2 atmosphere and stirred at ambient temperature. The products were analyzed by gas chromatography (GC) or GC/mass spectrometry (MS).

Results and Discussion

Syntheses. The ruthenium(II) complexes were synthesized with polypyridyl tetradentate ligands, TPA, 5-($MeOCO)_3$-TPA, TQA, and BPG, as shown in Figure 1. The new ligand, 5-($MeOCO)_3$-TPA, was prepared by a slight modification of the method reported for TQA.[19,29] The reaction of methyl 6-(bromomethyl)nicotinate and NH_4OH in THF gave

(27) Sheldrick, G. M. *SHELXL-97*; University of Göttingen: Göttingen, Germany, 1997.
(28) *International Tables for X-ray Crystallography*; Kynoch Press: Birmingham, England, 1974; Vol. IV.
(29) Tris(2-fluoro-6-pyridylmethyl)amine was also prepared from 2-fluoro-6-(bromomethyl)pyridine by an analogous procedure, although the yield was moderate (40%). Machkour, A.; Mandon, D.; Lachkar, M.; Welter, R. *Inorg. Chem.* **2004**, *43*, 1545−1550.

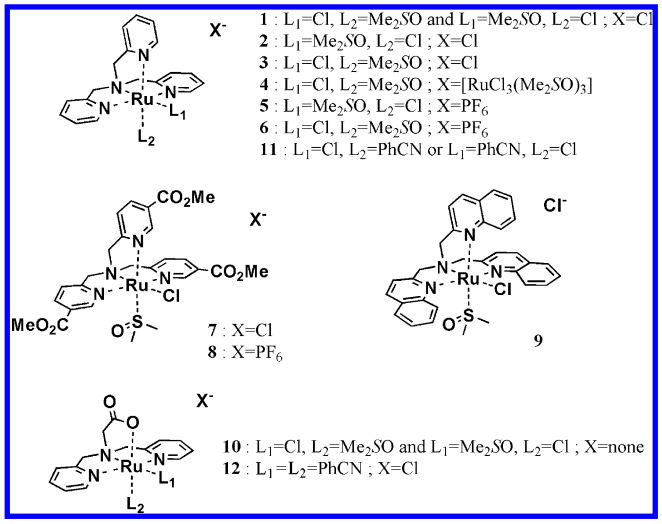

Figure 1. Structures of the complexes.

5-(MeOCO)$_3$-TPA in good yield (78%), which proved to be a convenient way for the syntheses of trisubstituted TPA derivatives with fewer steps and a better yield compared to a conventional method such as the reaction of 2 equiv of methyl 6-(bromomethyl)nicotinate with methyl 6-(aminomethyl)nicotinate. It is possible that it may be applicable to the syntheses of other TPA derivatives.

The chloro(dimethyl sulfoxide-κS)ruthenium(II) complexes, [RuCl(L)(Me$_2$*S*O)]$^{n+}$, were obtained from a reaction of the ligands and *cis*-[RuCl$_2$(Me$_2$SO)$_4$] by refluxing in methanol.[1,16,30] The Me$_2$*S*O ligands in these ruthenium(II) complexes are bound through S rather than O as shown below. With the TPA ligand, the chloride salt of the chloro(dimethyl sulfoxide)ruthenium(II) complex, [RuCl(TPA)(Me$_2$*S*O)]Cl, was obtained as a mixture of approximately equal amounts of two geometrical isomers: cis(Cl,N$_{amino}$) and trans(Cl,N$_{amino}$) isomers (**2** and **3**). This is in contrast to the selective formation of *cis*(Cl,N$_{amino}$)-[RuCl(TPA)(Me$_2$*S*O)]ClO$_4$ reported by Kojima et al., which may possibly have been due to the insolubility of the perchlorate salt of the cis isomer.[30] Recently, Bjernemose et al. have reported the selective preparation of *trans*(Cl,N$_{amino}$)-[RuCl(TPA)(Me$_2$*S*O)]PF$_6$ in high yield,[17] which is also inconsistent with our results. It is probably due to the higher reaction temperature employed in their studies: refluxing in ethanol. As mentioned below, the cis isomer could be isomerized to the trans one at higher temperatures, which accounts for the selective formation of the trans isomer at elevated temperatures. The trans and cis isomers of [RuCl(TPA)(Me$_2$*S*O)]Cl were separated by careful fractional recrystallization from methanol and ethyl acetate. The less soluble complex was the cis(Cl,N$_{amino}$) isomer **2**.

The ^{1}H NMR spectra of **2** and **3** show peaks of the methyl groups of Me$_2$*S*O at 2.84 and 3.42 ppm (in CD$_3$CN), respectively. Attempts to obtain good crystals of these complexes failed. However, a very small amount of complex **4** was obtained as crystals from the reaction mixture, which was found by X-ray analysis to be the trans(Cl,N$_{amino}$) isomer of the trichlorotris(dimethyl sulfoxide-κS)ruthenate, [RuCl$_3$(Me$_2$SO)$_3$]$^-$, salt as shown below. The trichlorotris(dimethyl sulfoxide-κS)ruthenate anion was probably produced from the starting complex during the reaction. The hexafluorophosphate salts of the *trans*- and *cis*-[RuCl(TPA)(Me$_2$*S*O)]$^+$ complexes were separated by fractional recrystallization from acetonitrile/diethyl ether to give complexes **5** and **6**, [RuCl(TPA)(Me$_2$*S*O)]PF$_6$. Complex **5**, which was less soluble and precipitated first as yellow crystals, was proven by X-ray analysis to be the cis(Cl,N$_{amino}$) isomer as shown below. The more soluble complex **6** was the trans(Cl,N$_{amino}$) isomer. On the other hand, the reaction of 5-(MeOCO)$_3$-TPA and *cis*-[RuCl$_2$(Me$_2$*S*O)$_4$] gave only one isomer of the chloro(dimethyl sulfoxide) complexes, [RuCl{5-(MeOCO)$_3$-TPA}(Me$_2$*S*O)]Cl **(7)** or [RuCl{5-(MeOCO)$_3$-TPA}(Me$_2$*S*O)]PF$_6$ **(8)**, even in the reaction mixture. This is in contrast to the fact that the reaction with TPA gave both cis and trans isomers, **2** and **3**. The reaction of *cis*-[RuCl$_2$(Me$_2$SO)$_4$] with the TQA ligand gave complex **9**, [RuCl(TQA)(Me$_2$*S*O)]Cl, which consisted of only one isomer of each.

The reaction with the BPG ligand gave complex **10**, which was a mixture of both the trans and cis isomers. However, the trans(Cl,N$_{amino}$) isomer of the chloro(dimethyl sulfoxide)ruthenium(II) complex is the sole product with 5-(MeOCO)$_3$-TPA and TQA as shown below, which is in contrast to the reactions with TPA or BPG. As for the complexes containing benzonitrile, the reaction of TPA and *trans*-[RuCl$_2$(PhCN)$_4$] gave the chloro(benzonitrile) complex, [RuCl(PhCN)(TPA)]Cl **(11)**. Complex **11** contained only one isomer, though the geometry was not determined. On the other hand, the reaction of BPG and *trans*-[RuCl$_2$(PhCN)$_4$] gave the bis(benzonitrile) complex, [Ru(BPG)(PhCN)$_2$]Cl (**12**). Although the yields of **11** and **12** were poor, no sign of other products was observed in the NMR and mass spectra of the crude products.

NMR Spectra. ^{1}H NMR spectral data of the complexes are listed in Table 3. The ^{1}H NMR spectra of the complexes prepared in this study are as expected for C_s symmetry, and one axial pyridylmethyl group and two in-plane pyridylmethyl groups are clearly distinguished. This is in contrast to the iron(II) complexes with TPA or its derivatives, which showed fluxional behavior.[31] The peaks of the methyl groups of Me$_2$*S*O of complexes **5** and **6** are observed at 3.43 and 2.85 ppm, respectively, and are almost identical with those of **2** and **3**. A methyl peak of Me$_2$*S*O observed at 2.86−2.93 ppm for **7** and **8**, which was similar to that of **3** and **6**, indicates that they are the trans(Cl,N$_{amino}$) isomers. The structure of **8** was confirmed by X-ray analysis as shown below. Kojima and colleagues reported that the reaction of 5-Me$_3$-TPA and *cis*-[RuCl$_2$(Me$_2$SO)$_4$] gave only *trans*(Cl,N$_{amino}$)-[RuCl(5-Me$_3$-TPA)(Me$_2$*S*O)]ClO$_4$ selectively, and the peak

(30) Kojima et al. reported that the selective formation of the one isomer of the chloro(dimethyl sulfoxide) complexes of TPA or 5-Me$_3$-TPA, *cis*(Cl,N$_{amino}$)-[RuCl(TPA)(Me$_2$*S*O)]ClO$_4$, and *trans*(Cl,N$_{amino}$)-[RuCl(5-Me$_3$-TPA)(Me$_2$*S*O)]ClO$_4$ in ref 14. See the text.

(31) (a) Diebold, A.; Hagen, K. S. *Inorg. Chem.* **1998**, *37*, 215−223. (b) Zang, Y.; Kim, J.; Dong, Y.; Wilkinson, E. C.; Appleman, E. H.; Que, L., Jr. *J. Am. Chem. Soc.* **1997**, *119*, 4197−4205. (c) Chen, K.; Que, L., Jr. *J. Am. Chem. Soc.* **2001**, *123*, 6327−6337.

Table 3. ^{1}H NMR Spectral Data of the Complexes[a]

	chemical shift/ppm (*J*/Hz)					
	C*H*$_2$	py-H3	py-H4	py-H5	py-H6	(C*H*$_3$)$_2$SO
TPA[b]	3.79 (s)	7.58 (d, 8)	7.69 (td, 8, 2)	7.17 (t, 6)	8.46 (d, 4)	
2, cis(Cl,N$_{amino}$)	4.69 (ax, s)	6.95 (ax, d, 8)	7.46−7.52 (ax, m)	7.16−7.25 (ax, m)	9.81 (ax, d, 6)	3.42 (s)
	4.79, 5.76 (ABq, 15)	7.46−7.51 (m)	7.73 (t, 8)	7.16−7.25 (m)	8.70 (d, 6)	
3, trans(Cl,N$_{amino}$)	4.53 (ax, s)	7.13 (ax, d, 8)	7.64 (ax, t, 8)	7.26−7.36 (ax, m)	9.69 (ax, d, 6)	2.84 (s)
	4.72, 5.39 (ABq, 15)	7.43 (d, 8)	7.76 (t, 8)	7.26−7.36 (m)	8.75 (d, 5)	
5-MeOCO-TPA[d]	3.97 (s)	7.63 (d, 8)	8.26 (dd, 8, 2)		9.14 (d, 2)	
8, trans(Cl,N$_{amino}$)	4.59 (ax, s)	7.24 (ax, d, 8)	8.16 (ax, dd, 8, 2)		10.22 (ax, d, 2)	2.86 (s)
	4.82, 5.44 (ABq, 16)	7.57 (d, 8)	8.27 (dd, 8,2)		9.20 (d, 2)	
5-Me$_3$-TPA[b]	3.71 (d, 2)	7.43−7.53 (m)	7.43−7.53 (m)	7.43−7.53 (m)	8.30 (d, 1)	
13, trans(Cl,N$_{amino}$)[b]	4.43 (ax, s)	7.00 (ax, d, 8)	7.47 (ax, dd, 8, 2)		9.53 (ax, s)	2.84 (s)
	4.59, 5.33 (ABq, 15)	7.29 (d, 8)	7.56 (dd, 8, 2)		8.57 (s)	
TQA[d]	4.13 (s)	7.74 (d, 8)	8.12 (d, 8)			
9, trans(Cl,N$_{amino}$)[c]	5.06 (ax, s)	7.80 (ax, d, 8)[e]	8.24 (ax, d, 8)[e]			2.93 (s)[d]
	5.23, 6.07 (ABq, 17)	7.67 (d, 8)[e]	8.48 (d, 8)[e]			
BPG[f]	3.78 (C*H*$_2$COO, s)	7.46−7.52 (m)	7.92 (d, 8)	7.46−7.52 (m)	8.54 (d, 5)	
	4.46 (C*H*$_2$py, s)					
10[d,g,h]	3.77 (A, C*H*$_2$COO, s)	7.24−7.31 (m)	7.62 (t, 7)	7.24−7.31 (m)	9.00 (d, 6)	3.67 (A, s)
	4.58, 5.94 (A, C*H*$_2$py, ABq, 14)					
	3.79 (B, C*H*$_2$COO, s)					3.62 (B, s)
	4.52, 5.82 (B, C*H*$_2$py, ABq, 14)					
11	4.64 (ax, s)	7.01 (ax, d, 8)	7.50 (ax, t, 8)	7.13 (ax, t, 8)	9.03 (ax, d, 6)	
	4.78, 5.43 (eq, ABq, 15)	8.08 (d, 8)	7.43 (t, 8)	7.26 (t, 8)	8.82 (d, 6)	
12	3.57 (C*H*$_2$COO, s)	8.05 (d, 8)	7.88 (t, 8)	7.44−7.88 (m)	8.89 (d, 6)	
	4.79, 4.96 (C*H*$_2$py, ABq, 15)					

[a] Measured in CD_3CN at room temperature unless noted otherwise. The protons noted ax are those of the axial pyridylmethyl group. For the data of complexes **1** and **5**−**7**, see the Experimental Section. [b] Reference 14. Measured in CD_3CN. [c] Measured in $(CD_3)_2SO$. [d] Measured in $CDCl_3$. [e] Quinolyl group. [f] Measured in D_2O. [g] Consisting of two isomers, A and B. See the text. [h] The chemical shifts of other quinolyl protons are observed at 8.06, 7.68, 7.50, and 7.77 ppm for 5H, 6H, 7H, and 8H, respectively.

of the methyl groups of Me_2SO was observed at 2.84 ppm.[30] The methylene protons of the axial pyridylmethyl groups were observed as a singlet at a higher magnetic field. On the other hand, the methylene protons of the in-plane pyridylmethyl groups appeared as an AB quartet because the C−H bonds point axial and equatorial. The large differences in the chemical shifts, from 0.62 to 0.97 ppm for the complexes with TPA-type ligands, between those axial and equatorial protons were observed. The large downfield shifts of the axial protons are possibly due to the van der Waals effect between the axial methylene protons and the Cl anion of the cis isomer or the O atom of the Me_2SO ligand as shown in the molecular structures of the complexes.[32] The chloro(dimethyl sulfoxide-κS) complex with BPG, [Ru(BPG)Cl(Me_2SO)]Cl (**10**), was a mixture of trans and cis isomers. Because the methylene protons were observed as two singlets at 3.77 and 3.79 ppm in **10** and one singlet at 3.57 ppm in **12**, the BPG ligand in these complexes has the symmetrical configuration with two pyridine rings trans to each other having C_s symmetry.

A peak of the methyl groups of Me_2SO of the TQA complex **9** is observed at 2.93 ppm (in $CDCl_3$), which shows that complex **9** is the trans(Cl,N$_{amino}$) isomer. The chemical shifts for the trans isomers are observed at 2.84−2.93 ppm, shifting upfield about 0.6 ppm compared to those of the cis isomers. Because the S-bound Me_2SO ligands of *cis*-[$RuCl_2(Me_2SO)_4$] and *cis*,*fac*-[$RuCl_2$(py)(Me_2SO)$_3$] show methyl peaks at 3.3−3.5 ppm similar to those of the cis isomers **2** and **5**,[33,34] the upfield shift observed in the trans isomers **3**, **6**−**9**, and *trans*(Cl,N$_{amino}$)-[RuCl(5-Me$_3$-TPA)(Me_2SO)]ClO_4 (**13**) can be attributed to the ring current effect of the pyridyl groups. The quinolyl protons, 8H, of **9** are observed at 9.67 and 11.02 ppm and show large downfield shifts from 7.77 ppm of the free ligand: 1.90 and 3.25 ppm for in-plane and axial positions, respectively. Both MM and QM calculations shown below exhibit that there are close contacts between the Cl ligand and 8H.

Molecular Structures of Complexes 4, 5, and 8. A single crystal of **4** was obtained as a salt with the [$RuCl_3(Me_2SO)_3$] anion unintentionally by the slow diffusion of ethyl acetate to a solution of the crude mixture of **2** and **3** in methanol.[15] Bjernemose et al. have reported the molecular structure of **6**.[17,35] An ORTEP drawing of the cation is shown in Figure 2, and selected bond lengths and angles are listed in Table 2. The Ru^{II} center of the cation of **4** had an octahedral geometry with four N atoms of the TPA ligand, a Cl anion, and a S of the S-bound Me_2SO ligand. It was found that **4** is the trans(Cl,N$_{amino}$) isomer: the chloride anion coordinates to the Ru center trans to the amino N and the Me_2SO ligand cis to the amino N. There were both trans and cis isomers in the reaction mixture; however, this isomer crystallized because of the low solubility of the trichlorotris(dimethyl sulfoxide-κS)ruthenate salt. The three Me_2SO ligands in the [$RuCl_3(Me_2SO)_3$]$^-$ anion coordinate to a Ru center by S atoms in the facial configuration. It is likely that the counteranion *fac*-[$RuCl_3(Me_2SO)_3$]$^-$ was formed by a nucleophilic attack of a Cl anion during the reaction. Yamamoto

(32) Nagata, W.; Terasawa, T.; Tori, K. *J. Am. Chem. Soc.* **1964**, *86*, 3746−3749.

(33) Evans, I. P.; Spencer, A.; Wilkinson, G. *J. Chem. Soc., Dalton Trans.* **1973**, 204−209.

(34) Alessio, E.; Calligaris, M.; Iwamoto, M.; Marzilli, L. G. *Inorg. Chem.* **1996**, *35*, 2538−2545.

(35) The crystal of **6** contains two independent complex ions in the asymmetric unit.

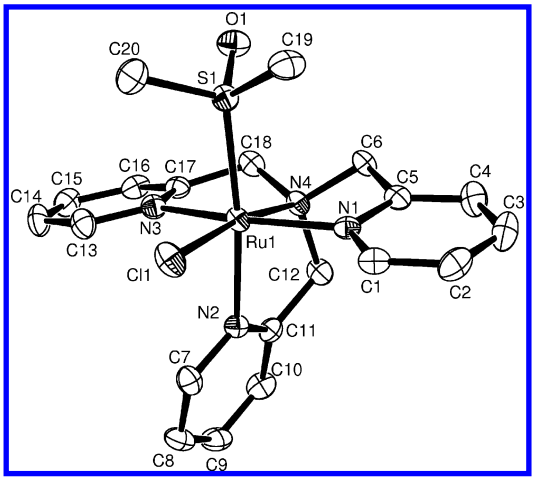

Figure 2. ORTEP drawing of the cation of **4**, *trans*(Cl,N_{amino})-[RuCl(TPA)(Me_2SO)]$^+$. Thermal ellipsoids are drawn at the 50% probability level.

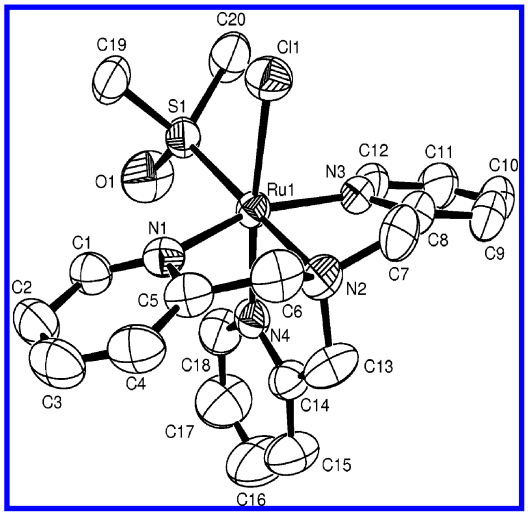

Figure 3. ORTEP drawing of the cation of **5**, *cis*(Cl,N_{amino})-[RuCl(TPA)(Me_2SO)]$^+$. Thermal ellipsoids are drawn at the 50% probability level.

and colleagues reported that the reaction of [$RuCl_2(Me_2SO)_4$] and bis(2,6-dimethoxyphenyl)phenylphosphine (BDMPP) afforded [BDMPP(CH_2Cl_2)][$RuCl_3(Me_2SO)_3$] as the main product, of which the three anions were in the facial configuration.[36]

A single crystal of **5**·$^1/_2$MeCN was obtained as the hexafluorophosphate salt by recrystallization from acetonitrile and toluene. An ORTEP drawing is shown in Figure 3, and selected bond lengths and angles are listed in Table 2. The presence of acetonitrile was confirmed by NMR and elemental analysis. The Ru^{II} center of **5** had an octahedral geometry with four N atoms of the TPA ligand, a Cl anion, and a S of the S-bound Me_2SO ligand. It was found that **5** is a cis(Cl,N_{amino}) isomer: the Cl anion coordinates to the Ru center cis to the amino N and the Me_2SO ligand trans to the amino N.

A good crystal of **8** suitable for X-ray analysis was obtained by the slow diffusion of ethanol to a solution of **8** in acetone. An ORTEP drawing is shown in Figure 4, and

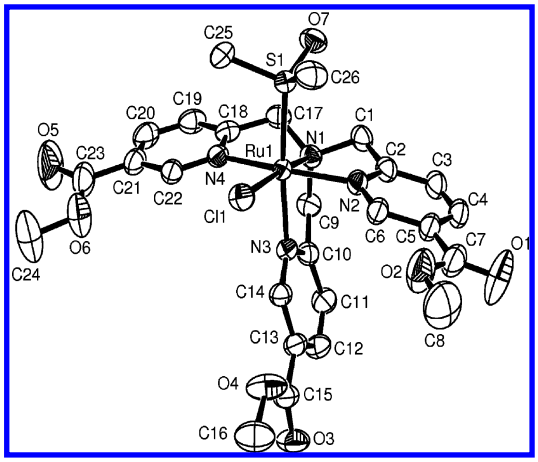

Figure 4. ORTEP drawing of the cation of **8**, *trans*(Cl,N_{amino})-[RuCl{5-($MeOCO)_3$-TPA}(Me_2SO)]$^+$. Thermal ellipsoids are drawn at the 50% probability level.

selected bond lengths and angles are listed in Table 2. It was found that **8** is a trans(Cl,N_{amino}) isomer: the Cl anion coordinates to the Ru center trans to the amino N and the dimethyl sulfoxide (DMSO) ligand cis to the amino N. The methoxycarbonyl groups were approximately in the planes of the pyridyl groups, and the C═O groups were anti to the N atoms of the pyridyl groups in the crystal. The dihedral angles of O═C−C(5-pyr)−C(4-pyr) range from 1.5(5)° to 12.6(6)°.

Selected bond lengths, angles, and torsional angles of complexes **4**, **5**, and **8** are listed in Table 4, including those of $\mathbf{6_A}$, $\mathbf{6_B}$,[17,35] and **13**.[14] Bond lengths of Ru−N_{amino} in **4** and **8** are 2.070(3) and 2.0753(18) Å, respectively, which are similar to those in $\mathbf{6_A}$, $\mathbf{6_B}$, and **13** of 2.082(3), 2.080(2), and 2.062(4) Å, respectively. The average of the Ru−N_{amino} bond lengths of the trans isomers is 2.074(4) Å. The bond length of Ru−N_{amino} in the cis isomer **5** is 2.095(2) Å, which is slightly longer than those in the trans isomers. On the other hand, the bond length between Ru and the N atom of the axial pyridyl group in the cis isomer **5** is 2.065(2) Å, which is shorter than those in the four trans isomers: the average is 2.103(1) Å [2.099(2)−2.106(3) Å]. The elongation of the Ru−N bond of the axial pyridyl group in the trans isomers is probably due to the trans effect of the Me_2SO ligand. The S−Ru−Cl bond angle in the cis isomer **5** is 85.75(3)°, which is smaller than those in the four trans isomers: 87.36(7)−88.87(3)°. The proximity of the Me_2SO ligand to the axial pyridyl group in the cis isomer **5** may result in the decrease of the S−Ru−Cl bond angle. In fact, the interatomic distance between the O atom of the Me_2SO ligand and the ortho H atom of the axial pyridyl group O1···H18 is 2.253 Å, which is much shorter than the sum of the van der Waals radii. In the structural study of *cis*-[RuCl($bpy)_2$(Me_2SO)]X (X = PF_6 and I), the H bondings between the O atom of the Me_2SO ligand and the ortho proton of the pyridyl group have been reported: the O···H distance is 2.26 Å.[37] The steric interaction derived from the Me_2SO ligand is partially reduced in the trans isomers. The average interatomic distance between

(36) Yamamoto, Y.; Sugawara, K.; Aiko, T.; Ma, J.-F. *J. Chem. Soc., Dalton Trans.* **1999**, 4003−4008.

(37) Hasek, D.; Inoue, Y.; Everitt, S. R. L.; Ishida, H.; Kunieda, M.; Drew, M. G. B. *J. Chem. Soc., Dalton Trans.* **1999**, 3701−3709.

Table 4. Selected Bond Lengths (Å), Angles (deg), Torsional Angles (deg), and Interatomic Distances (Å) for **4**, **6**, **8**, **13**, and **5**[a]

	complex					
	4	**6**$_A$[b]	**6**$_B$[b]	**8**	**13**[c]	**5**
Ru−Cl	2.4321(9)	2.430(1)	2.420(1)	2.4258(5)	2.423(2)	2.4319(9)
Ru−S	2.2385(10)	2.251(1)	2.258(1)	2.2587(5)	2.236(2)	2.2653(8)
Ru−N_{amino}	2.070(3)	2.082(3)	2.080(2)	2.0753(18)	2.062(4)	2.095(2)
Ru−N_{ax}	2.106(3)	2.101(2)	2.099(2)	2.1029(18)	2.104(5)	2.065(2)
Ru−N	2.078(3)	2.087(3)	2.079(2)	2.0594(18)	2.066(4)	2.079(2)
	2.060(3)	2.093(2)	2.060(2)	2.0776(18)	2.090(4)	2.091(2)
S−O	1.480(2)	1.492(2)[d]	1.491(2)[d]	1.4918(17)	1.485(4)	1.479(3)
S−Ru−Cl	88.87(3)	87.75(6)[d]	88.32(6)[d]	88.01(2)	87.36(7)	85.75(3)
O−S−Ru−Cl	161.71(3)	177.70(3)[d]	178.23(3)[d]	171.51(9)	179.79(4)[d]	174.26(16)
N_{amino}−C−C−N_{ax}	29.24(8)	21.15(8)[d]	4.93(8)[d]	28.6(3)	18.5(1)[d]	1.8(5)
O···H_{mt}	2.381	2.382	2.363	2.447	2.225	
	2.597	2.588	2.502	2.467	2.369	
O···H_{pyax}	2.253					
Cl···H_{pyax}	2.692	2.625	2.641	2.640	2.698	
Cl···H_{mt}	2.751					
	2.851					

[a] N_{amino} = amine nitrogen, N_{ax} = axial pyridyl nitrogen, N = pyridyl nitrogen in plane, H_{mt} = methylene proton of the pyridylmethyl group in plane, H_{pyax} = ortho proton of the axial pyridyl group. [b] Reference 17. [c] Reference 14. [d] Calculated by VENUS developed by Dilanian and Izumi.

the O atom and the methylene protons of the TPA ligand is 2.435 Å (2.225−2.597 Å) in **4**, **6**, **8**, and **13**, although they are still shorter than the sum of the van der Waals radii. Complexes **5** and **6**$_B$ are found to be approximately C_s symmetrical. The axial pyridyl group is almost in the symmetrical plane: the N_{amino}−C−C(2-pyr)−N_{ax} torsional angles are 1.8(5)° in **5** and 4.93(8)° in **6**$_B$. On the other hand, other complexes are slightly distorted from the C_s symmetry: the torsional angles in the axial chelate ring are 29.24(8)° in **4**, 29.1(13)° and 28.6(3)° in **8**, 21.15(8)° in **6**$_A$, and 18.5(1)° in **13**.

The bond lengths of S−O in the Me_2SO ligand are 1.480(2), 1.479(3), and 1.4918(17) Å in **4**, **5**, and **8**, respectively. The average is 1.484(4) Å. The S−O bond lengths of free DMSO were reported to be 1.513(5) Å for the crystal structure of DMSO measured at 5 °C and 1.50(1) Å for liquid DMSO determined by X-ray diffraction.[38,39] Calligaris and Carugo reported that the mean S−O bond length of the free solvate DMSO in the crystal structures was 1.492(1) Å with exclusion of the values of the low temperature and of the compounds involved in strong H bonds, and the mean S−O bond length of the S-bonded (dimethyl sulfoxide)ruthenium(II) complexes in the crystals was 1.478(1) Å.[40] Kojima and colleagues have claimed that the S−O bond in **13**, 1.485(5) Å, was elongated because of a strong π-back-donation from dπ of the Ru^{II} ion to pπ^* of the S═O bond.[41] However, the S−O bond lengths in **4**, **5**, and **13** are close to the mean S−O bond value of the S-bonded (dimethyl sulfoxide)ruthenium(II) complexes in the crystals. The Ru−S bond lengths in **4**, **5**, and **8** are 2.2385(10), 2.2653(8), and 2.2587(5) Å, respectively. The Ru−S bond lengths in **5** and **8** are close to the reported mean Ru−S bond length of 2.265(3) Å,[40] while that in **4** was shorter than the mean value. The S−O bonds in the complexes **4**, **5**, and **8** were directed approximately anti to the Cl anion coordinated cis to the Me_2SO ligand, which is possibly due to the electrostatic repulsion between the Cl anion and the O atom of the Me_2SO ligand. The O−S−Ru−Cl torsional angles in **4**, **5**, and **8** are 161.73(3)°, 174.26(16)°, and 171.51(9)°, respectively, so that the O atom of the Me_2SO ligand is anti to the Cl ligand. The rotational barriers around the Ru−S bond were estimated to be 9−14 kcal/mol by MM calculations as shown in Figure 5. The coordinating Cl ions are in proximity to the axial methylene protons of the pyridylmethyl groups in **5**, 2.751 and 2.851 Å, and to the ortho proton of the axial pyridyl group in **4** and **8**, 2.692 and 2.640 Å, respectively. The Cl···H interatomic bond distances are much shorter than the sum of the van der Waals radii.

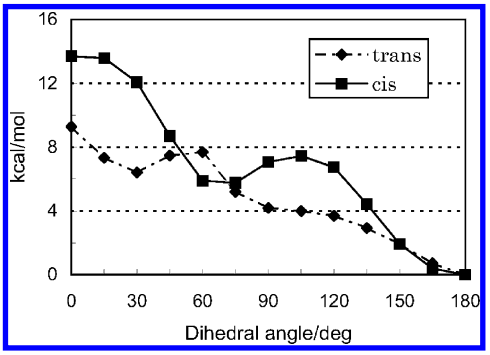

Figure 5. Rotational barriers of the S-bonded DMSO ligands of *trans*- and *cis*(Cl,N_{amino})-[RuCl(TPA)(Me_2SO)]$^+$ complexes.

Although 5-Me_3-TPA and 5-$(MeOCO)_3$-TPA have the electron-donating and -withdrawing substituents on the 5 positions of the pyridyl groups, the molecular structures of the trans(Cl,N_{amino}) isomers of TPA, 5-Me_3-TPA, and 5-$(MeOCO)_3$-TPA show no notable difference. The geometry around the Ru center does not seem to be affected significantly by the steric and electronic effects of the substituents on the 5 positions of the pyridyl groups.

(38) Thomas, R.; Shoemaker, C. B.; Eriks, K. *Acta Crystallogr.* **1966**, *21*, 12−20.
(39) Itoh, S.; Ohtaki, H. *Z. Naturforsch.* **1987**, *42a*, 858−862.
(40) Calligaris, M.; Carugo, O. *Coord. Chem. Rev.* **1996**, *153*, 83−154.
(41) According to Kojima et al. in ref 14, the S−O bond length of free DMSO was 1.47 Å: *Kagaku Binran, Kisohen*; The Chemical Society of Japan, Maruzen: Tokyo, Japan, 1966; Vol. II, p 1222. However, the value was revised to be 1.485 Å in: *Kagaku Binran, Kisohen*, 3rd ed.; The Chemical Society of Japan, Maruzen: Tokyo, Japan, 1984; Vol. II, p 658.

Scheme 1

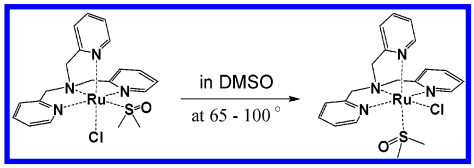

Thermal Isomerization. The *cis*(Cl,N_{amino})-[RuCl(TPA)-(Me_2SO)]$^+$ complex **2** is found to be thermodynamically unstable compared to the trans isomer **3**. The cis isomer isomerized to the trans one in a DMSO solution at 65−80 °C with first-order kinetics (Scheme 1), which was followed by UV/visible spectra (Figure S1 in the Supporting Information). The spectral change of the cis isomer **2** at 65−80 °C was observed with isosbestic points at 387 and 265 nm, as shown in Figure 6, although the trans isomer **3** showed no change even at 100 °C. The rate constants were 4.7×10^{-6}, 8.6×10^{-6}, 2.2×10^{-5}, and 4.5×10^{-5} s^{-1} at 65, 70, 75, and 80 °C, respectively. From Eyring's rate equation,[42] values of $\Delta H^{\ddagger} = (37 \pm 1)$ kcal/mol and $\Delta S^{\ddagger} = +(24 \pm 4)$ cal/mol were determined (Figure S2 in the Supporting Information). The ^{1}H NMR measurements clearly indicate that the peaks of the cis isomer decreased during heating at 100 °C and those of the trans isomer evolved. After 6 h, the peaks of the cis isomer disappeared, and the spectrum became identical with that of the trans isomer, as shown in Figure S3 in the Supporting Information. Because the cis isomer is not detectable (<1%) in NMR measurements of the equilibrated mixture, the trans isomer is estimated to be 3.4 kcal/mol more stable than the cis isomer at 100 °C.

The preparation of the chloro(dimethyl sulfoxide) complex, [RuCl(TPA)(Me_2SO)]$^+$, by the reaction of TPA and *cis*-[$RuCl_2(Me_2SO)_4$] in methanol was repeated many times. However, a mixture of the cis and trans isomers was always obtained.[43] These results may have been caused by kinetic control, although the reaction mechanism is uncertain. The selective synthesis of the trans isomer by a similar reaction in ethanol reported by Bjernemose et al. was possibly due to simultaneous isomerization in the reaction conditions.

MM and QM Calculations. We have carried out MM and QM calculations using DFT of the chloro(dimethyl sulfoxide) complexes with TPA or its derivative. This showed that the trans isomers are much more stable than the cis isomers (Tables 5 and S1 in the Supporting Information). MM calculations using CAChe show that the energy difference is 6.03 kcal/mol for the TPA complexes and 5.90 kcal/mol for the 5-$(MeOCO)_3$-TPA complexes. DFT calculations using B3LYP functionals with geometry optimization show that the energy differences are 5.58 and 5.43 kcal/mol, respectively, for the TPA complexes and the 5-$(MeOCO)_3$-TPA complexes by using the LANL2DZ basis set (or 6.62 and 5.81 kcal/mol, respectively, by using the 3-21G** basis set). These results are in agreement with the experiments. In the cis TPA isomer, the O−S−Ru−Cl torsional angle is 154.69° and the O···H interatomic distance is 2.091 Å (2.253 Å is the observed value) between the O atom of the Me_2SO ligand and the H atom of the axial pyridyl group, which suggests a strong steric repulsion between the O atom of the Me_2SO ligand and the axial pyridyl group. Similarly, the cis(Cl,N_{amino}) isomer of [RuCl(TQA)(Me_2SO)]$^+$ is considerably less stable than the trans(Cl,N_{amino}) isomer. The trans isomer of [RuCl(TQA)(Me_2SO)]$^+$ is 3.03 kcal/mol more stable than the cis isomer by MM calculations and 4.57 kcal/mol more stable by B3LYP/LANL2DZ (or 6.47 kcal/mol by B3LYP/3-21G**) calculations because of steric repulsion between the Me_2SO ligand and the quinolyl groups of TQA in the cis isomer. In fact, the complex *cis*-[RuCl(TQA)-(Me_2SO)]$^+$ has not been obtained.

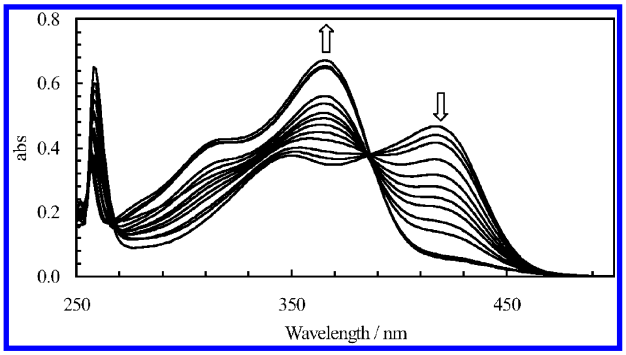

Figure 6. UV/visible spectral change of complex **2**, *cis*(Cl,N_{amino})-[RuCl-(TPA)(Me_2SO)]$^+$, in Me_2SO at 80 °C.

Table 5. Energy Differences (kcal/mol) between the trans(Cl,N_{Amino}) and cis(Cl,N_{Amino}) Isomers of [RuCl(L)(Me_2SO)]$^+$ Complexes[a]

L	MM2	DFT[b]
TPA	+6.03	+5.58 (+6.62)
5-$(MeOCO)_3$-TPA	+5.90	+5.43 (+5.81)
TQA	+3.03	+4.57 (+6.47)

[a] Energy difference (kcal/mol) = E(cis) − E(trans). [b] Calculated by B3LYP/LANL2LZ. Results using basis set 3-21G** are given in parentheses.

Electrochemistry. CVs of the complexes were measured in MeCN with 0.1 M Et_4NClO_4, and redox potentials were determined relative to an Fc/Fc^+ couple as 0 V. CV data are summarized in Table 6, and CVs of complexes **2** and **3** are shown in Figure 7.[44] All ruthenium complexes measured show a reversible redox couple due to the Ru^{II}/Ru^{III} couple at +0.41 to +0.94 V except for complex **10**, which is a

(42) Wilkins, R. G. *Kinetics, Mechanism of Reactions of Transition Metal Complexes*, 2nd ed.; VCH: Weinheim, Germany, 1991.

(43) The thermal isomerization experiment was attempted in MeOH, either. However, after heating at 60 °C for 5 h, only a small change in the UV/visible absorption spectrum, which did not correspond to that of the isomerization reaction, was observed. It is assumed that the thermal isomerization rate in MeOH is very slow and/or the ligand substitution by a solvent molecule proceeded simultaneously in MeOH.

(44) A quasi-reversible redox couple at +0.03 V was observed in the CV of complexes **2** and **5**, which shifted negatively from the Ru^{II}/Ru^{III} couple (Figure 7a). Kojima et al. have reported a reversible redox couple observed at +0.04 V in the CV of the *cis*(Cl,N_{amino})-[RuCl-(TPA)(Me_2SO)]ClO_4 complex, and this redox couple is suspected to be the linkage isomer of **2** and **5** with an O-bound DMSO ligand in ref 30. According to Kojima et al., the linkage isomerization of the DMSO ligand takes place in the cis(Cl,N_{amino}) isomer of the [RuCl-(TPA)(Me_2SO)]$^+$ complex. It is noteworthy that all of the trans isomers **3**, **6**−**8**, and **13**[30] show no detectable wave around 0 V. Kojima et al. have explained the absence of the electrochemical process in the CV of the *trans*(Cl,N_{amino})-[RuCl(5-Me_3-TPA) (Me_2SO)]$^+$ complex by the electronic effect of the 5-methyl substituents of 5-Me_3-TPA, which increase the electron density at the Ru center. However, that is not the case because the complex having 5-$(MeOCO)_3$-TPA, which has the substituents with the opposite electronic effect, showed no peak attributable to the linkage isomerization.

Table 6. Redox Potentials of Complexes **2**−**12** Measured in CH_3CN[a]

complex	E_a	E_c	$E_{1/2}$
cis(Cl, N_{amino})-[RuCl(TPA)-(Me_2SO)]Cl (**2**)	+0.63[b]	+0.56[b]	+0.60[b]
trans(Cl,N_{amino})-[RuCl(TPA)-(Me_2SO)]Cl (**3**)	+0.60[b]	+0.53[b]	+0.56[b]
cis(Cl,N_{amino})-[RuCl(TPA)-(Me_2SO)]PF_6 (**5**)	+0.66	+0.59	+0.62
trans(Cl,N_{amino})-[RuCl(TPA)-(Me_2SO)]PF_6 (**6**)	+0.61	+0.54	+0.57
trans(Cl,N_{amino})-[RuCl{5-$(MeOCO)_3$TPA}-(Me_2SO)]PF_6 (**8**)	+0.80	+0.74	+0.77
trans(Cl,N_{amino})-[RuCl(5-Me_3-TPA)-(Me_2SO)]ClO_4 (**13**)			+0.52[c]
trans(Cl,N_{amino})-[RuCl(TQA)-(Me_2SO)]Cl (**9**)	+0.97	+0.92	+0.94
[Ru(BPG)Cl(Me_2SO)] (**10**)	+0.20	+0.12	+0.16
[RuCl(PhCN)(TPA)]Cl (**11**)	+0.45	+0.37	+0.41
[Ru(BPG)$(PhCN)_2$]Cl (**12**)	+0.61	+0.51	+0.56

[a] Potentials were determined relative to a Fc/Fc^+ couple as 0 V; measured at ambient temperature in MeCN under N_2; electrolyte, 0.1 M Et_4NClO_4; [complex] = 1.3 mM; working electrode = Pt, counter electrode = Pt; scan rate = 500 mV/s. [b] Scan rate = 100 mV/s. [c] Kojima, T.; Amano, T.; Ishii, Y.; Ohba, M.; Okaue, Y.; Matsuda, Y. *Inorg. Chem.* **1998**, *37*, 4076−4085. Measured in 0.1 M [(n-Bu)$_4$N]ClO_4/MeCN.

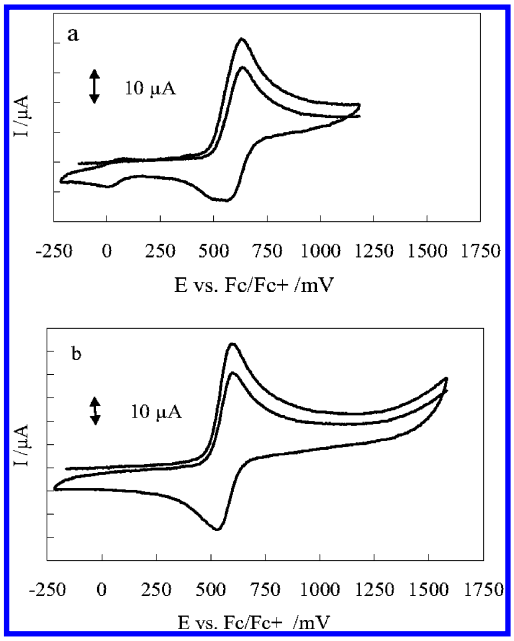

Figure 7. CVs of (a) complex **2**, *cis*(Cl,N_{amino})-[RuCl(TPA)(Me_2SO)]Cl, and (b) complex **3**, *trans*(Cl,N_{amino})-[RuCl(TPA)(Me_2SO)]Cl, at ambient temperature in CH_3CN (500 mV/s, 0.1 M Et_4NClO_4, mV vs Fc/Fc^+).

neutral complex, showing at +0.16 V. The redox potentials of the cis isomers **2** and **5** are slightly more positive than those of the trans isomers **3** and **6**. As for the substituent effects in TPA ligands, the redox potentials lie in the order 5-$(MeOCO)_3$-TPA > TPA > 5-Me_3-TPA. This is due to the electronic property of the substituents in TPA; i.e., the electron-withdrawing group results in the higher redox potential because the higher oxidation state of the ruthenium complex is destabilized by electron-withdrawing 5-position substituents on the TPA ligand. A similar tendency has been reported for a series of ruthenium complexes with substituted bipyridine derivatives[45] and iron complexes with TPA derivatives.[46] The redox potential of **9** is about 0.4 V more positive than that of **6**, which is probably due to both the electronic effect and the distortion from the octahedron caused by the quinolyl rings. Similar positive shifts of the redox potentials were observed for the ruthenium complexes with 2,2′-biquinoline.[47]

Table 7. Catalytic Oxidation of Adamantane by Ruthenium Complexes[a]

		yield/%[b]				
run	catalyst	1-ol	2-ol	2-one	1-Cl	diol
1	**1**	63	trace	trace	6	24
2[c]	**5**	57	2	trace	3	4
3[d]	**5**	21	3	trace	5	nd[k]
4[c]	**6**	77	4	trace	3	9
5[d]	**6**	58	3	trace	4	nd[k]
6[e]	**6**	88	2	trace	4	trace
7	**7**	46	0	trace	4	52
8[f]	**7**	76	0	2	2	1
9[g]	**7**	5	0	trace	1	88
10[h]	**7**	26	1	2	3	nd[k]
11[i]	**7**	10	0	0	1	0
12[j]	**7**	39	0	1	1	50
13	**9**	63	4	1	2	nd[k]
14	none	7	1	1	1	1

[a] The reaction was performed in $CHCl_3$ at room temperature for 24 h unless stated otherwise: [substrate] = 4×10^{-2} mol/L, [catalyst] = 2×10^{-4} mol/L, [MCPBA] = 6×10^{-2} mol/L. Abbreviation: diol = adamantane-1,3-diol. [b] Determined by GC/MS analyses with an internal standard based on the substrate. [c] [catalyst] = 4×10^{-4} mol/L. [d] [catalyst] = 4×10^{-4} mol/L; [MCPBA] = 3×10^{-2} mol/L. [e] The catalyst was added in three portions during 48 h. [f] [substrate] = 6×10^{-2} mol/L. [g] [MCPBA] = 1.8×10^{-1} mol/L. [h] t-BuOOH was used instead of MCPBA. [i] PhIO was used instead of MCPBA. [j] In 1,2-dichloroethane. [k] nd = not determined.

Catalytic Oxidation of Alkane. Metal-catalyzed alkane oxidation utilizing ruthenium complexes has been studied. Ruthenium complexes with a tetradentate ligand such as TPA have shown considerable activity on the catalytic oxidation of alkanes.[1,11] Oxidation of adamantane catalyzed by the ruthenium complexes having a TPA or BPG in the presence of MCPBA was examined using **1** and **10**−**12** in various solvents, as given in Table S5 in the Supporting Information. It was found that 1-adamantanol was the main product and the reactivity was dependent on the solvent used: $CHCl_3$ > CH_2Cl_2 > MeCN = Me_2CO. The reaction favored solvents of halogenated C, such as dichloromethane and chloroform.[1] However, 1-chloroadamantane was also obtained possibly as a result of a free-radical process involving solvent molecules.[48] Further, the catalytic oxidation of adamantane employing various chloro(dimethyl sulfoxide-κS)ruthenium complexes **1**, **5**−**7**, and **9** with a TPA-type ligand, TPA, 5-$(MeOCO)_3$-TPA, or TQA, was examined in chloroform, with the results summarized in Table 7. An excess amount of MCPBA was employed in these experiments because concurrent decomposition of MCPBA was observed.[49] In the

(45) Elliott, C. M.; Hershenhart, E. J. *J. Am. Chem. Soc.* **1982**, *104*, 7519−7526.
(46) Chen, K. C.; Que, L., Jr. *J. Am. Chem. Soc.* **2001**, *123*, 6327−6337.
(47) Vlcek, A. A.; Dodsworth, E. S.; Pietro, W. J.; Lever, A. B. P. *Inorg. Chem.* **1995**, *34*, 1906−1913.
(48) Bravo, A.; Fontana, F.; Minisci, F.; Serri, A. *Chem. Commun.* **1996**, 1843−1844.
(49) Adamantane is oxidized in the absence of the catalyst by MCPBA in a free-radical process as shown in run 14; however, the contribution of the noncatalyzed process can be considered to be negligible. The oxidation of adamantane by MCPBA has been reported by Bravo and co-workers.[48]

Table 8. Catalytic Oxidation of Cyclooctane and Ethylbenzene by Ruthenium Complexes[a]

		yield/%[b]			yield/%[b]		
catalyst	run	cyclooctanone	cyclooctanol	run	acetophenone	1-phenylethanol	1-chloro-1-phenylethane
1	1	27	1	7	2	0	8
6	2	25	5	8	8	6	nd[c]
7	3	50	1	9[d]	22	1	4
9	4	17	4				
10	5	8	5				
none	6	1	1	10	1	0	0

[a] The reaction was performed in $CHCl_3$ at room temperature for 24 h: [substrate] = 4×10^{-2} mol/L, [catalyst] = 4×10^{-4} mol/L, [MCPBA] = 6×10^{-2} mol/L. [b] Determined by GC or GC/MS analyses with an internal standard based on the substrate. [c] nd = not determined. [d] [catalyst] = 2×10^{-4} mol/L.

Scheme 2

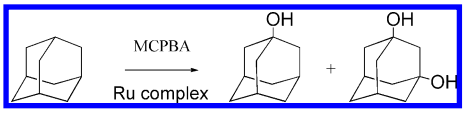

reaction of adamantane, a tertiary C atom(s) was (were) selectively oxidized, and 1-adamantanol and adamantane-1,3-diol were obtained in good to excellent yield (Scheme 2). The selectivity for oxidation of tertiary versus secondary C−H was found to be very high: 3°/2° ratios[50] were 132 and 114 for runs 6 and 8 catalyzed by **6** and **7**, respectively, and almost no 2-adamantanol and 2-adamantanone were obtained in runs 7 and 9 catalyzed by **7**.[51] The 1-adamantanol produced by the catalytic oxidation was further oxidized to yield adamantane-1,3-diol, when an excess amount of MCPBA was present (runs 7, 9, and 12). An independent experiment showed that oxidation of 1-adamantanol catalyzed by **7** under the same conditions yielded adamantane-1,3-diol in 61% yield with **7** and 23% with **1**. Using the cis isomer (**5**) and the trans isomer (**6**) of the [RuCl(TPA)-(Me_2SO)] complex individually, it was found that the trans isomer (**6**) was more active as the catalyst than the cis isomer (run 2 vs 4 and run 3 vs 5). Recently, Jitsukawa et al. have proposed that the *trans*(Cl,N_{amino})-Ru=O species derived from the chloro(dimethyl sulfoxide)ruthenium complex having a TPA-type ligand is more active on C−H bond activation than the corresponding *cis*(Cl,N_{amino})-Ru=O species, which is probably a result of the trans influence.[11e] The activity of the trans isomer (**6**) could also be explained by the trans influence because the DMSO ligand might be substituted with an MCPBA to give the *trans*(Cl,N_{amino})-Ru=O species. The formation of 1-chloroadamantane decreased in 1,2-dichloroethane (run 12) because it is well-known that the abstraction of Cl atoms from solvent molecules occurs more easily in chloroform.[48] The oxidation of cyclooctane and ethylbenzene was also examined (Table 8). Ketones, cyclooctanone, and acetophenone were the main products,[52] and it was found that the complex **7** having three methoxycarbonyl groups (MeOCO) at the pyridine 5 position of TPA was the most active catalyst. The MeOCO group at the 5 position, which is an electron-withdrawing group,[53] seems to enhance the catalytic activity on the oxidation of alkane. The enhancement is possibly due to the trans influence of the MeOCO group in the pyridine trans to the oxo. Studies of the catalyst using TPA derivatives having electron-withdrawing group(s) have been few. The catalytic activity of iron complexes with TPA derivatives having one or two methoxycarbonyl group(s), 5-(MeOCO)-TPA and 5-$(MeOCO)_2$-TPA, on alkane oxidation in the presence of H_2O_2 was studied; however, no distinctive effect was reported.[46] Recently, Jitsukawa et al. reported that the ruthenium complexes with the TPA-type ligands having neopentylamino group(s), an electron-donating group, at the 6 position of the pyridyl groups were the more active catalysts on oxidation of adamantane compared to the complexes with TPA or the TPA derivatives with electron-withdrawing 6-pivalamide group(s).[11d,e] They employed monochloro- or dichlororuthenium(II) complexes with 6-pivalamide group(s) and dichlororuthenium(III) complexes with 6-neopentylamino group(s) for the oxidation catalyst in the presence of PhIO as the cooxidant. The difference in the reaction conditions and the steric effect of the substituent at the 6 position may account for the inconsistency in the catalytic activity.[54]

Oxidation of *cis*-decalin by H_2O_2−$FeSO_4$ proceeds with isomerization, giving both *cis*- and *trans*-decal-9-ol (cis/trans = 23/77), which suggests the generation of long-lived alkyl radicals.[55] On the other hand, it has been reported that the ruthenium porphyrins catalyzed the oxidation of *cis*-decalin to *cis*-decal-9-ol with complete retention.[51b,56] Oxidation of *cis*-decalin catalyzed by complex **7** has been examined. It was revealed that *cis*-decalin was hydroxylated with retention of the configuration (cis/trans = 97/3; conversion = 98%). This is in contrast to the fact that the oxidation of *cis*-decalin by MCPBA in the absence of the catalyst proceeded with the concurrent isomerization (cis/trans = 71/29; conversion

(50) /([2-ol] + [2-one]) ratio taking account of the number of C−H bonds in a group.

(51) Selective hydroxylation of adamantane at tertiary C atom(s) catalyzed by ruthenium porphyrin complexes was reported: (a) Ohtake, H.; Higuchi, T.; Hirobe, M. *J. Am. Chem. Soc.* **1992**, *114*, 10660−10662. (b) Groves, J. T.; Bonchio, M.; Carofiglio, T.; Shalyaev, K. *J. Am. Chem. Soc.* **1996**, *118*, 8961−8962.

(52) No Baeyer−Villiger product was observed in the oxidation of cyclooctane, although ϵ-caprolactone was obtained in the oxidation of cyclohexane: Yamaguchi, M.; Murakami, N.; Yamagishi, T., unpublished results.

(53) Hansch, C.; Leo, A.; Taft, R. W. *Chem. Rev.* **1991**, *91*, 165−195.

(54) We have studied oxygenation of adamantane catalyzed by various kinds of *trans*(Cl,N_{amino})-[RuCl(5-R_3-TPA)(Me_2SO)]Cl complexes and found that the complex with 5-(benzylamide)-TPA was less reactive than that with TPA although that with 5-(benzyloxycarbonyl)-TPA was as reactive as that with 5-(methoxycarbonyl)-TPA: Yamaguchi, M.; Izawa, S.; Yamagishi, T., unpublished results.

(55) Shul'pin, G. B.; Süss-Fink, G.; Shul'pina, L. S. *Chem. Commun.* **2000**, 1131−1132.

(56) (a) Higuchi, T.; Hirobe, M. *J. Mol. Catal. A: Chem.* **1996**, *113*, 403−422. (b) Shingaki, T.; Miura, K.; Higuchi, T.; Hirobe, M.; Nagano, T. *Chem. Commun.* **1997**, 861−862. (c) Groves, J. T.; Nemo, T. E. *J. Am. Chem. Soc.* **1983**, *105*, 6243−6248.

= 20%). High 3°/2° ratios in the oxidation of adamantane and high stereoselectivity in the oxidation of *cis*-decalin suggest the involvement of a metal-based oxidant that generates short-lived alkyl radicals.[46,57]

Conclusion

A series of ruthenium(II) complexes having a tetradentate ligand, TPA, and its derivatives, 5-$(MeOCO)_3$-TPA and TQA, have been prepared and characterized in both solution and solid states. The chloro(dimethyl sulfoxide-κS) complexes with a TPA derivative seem to prefer the trans-(Cl,N_{amino}) configuration, except that with TPA, which was obtained as a mixture of the cis and trans isomers. A mixture of both chloride and the hexafluorophosphate salt of the configuration isomers of chloro(dimethyl sulfoxide-κS)(TPA) complexes was successfully separated by fractional recrystallization. The cis(Cl,N_{amino}) isomer with TPA was found to be much less stable than the trans one because it isomerized in DMSO at high temperatures (65−100 °C), which was supported by MM and DFT calculations. The chloro(dimethyl sulfoxide-κS) complexes with TPA or its derivatives were found to be an efficient catalyst for the oxygenation of alkanes. The tertiary C atom was selectively oxidized to give 1-adamantanol, and extremely high 3°/2° ratios were observed. The most active catalyst was *trans*-(Cl,N_{amino})-[RuCl{5-$(MeOCO)_3$-TPA}(Me_2SO)]PF_6. High stereoselectivity was observed in the oxidation of *cis*-decalin to give *cis*-decal-9-ol with complete retention of the configuration. The involvement of a metal-based oxidant that generates short-lived alkyl radicals is suggested.

Acknowledgment. We thank Prof. Ken Sakai for helpful advice on X-ray diffraction analysis. We thank Dr. Takahiko Kojima for helpful discussion. We also thank Shigeru Iokawa, Noriyasu Murakami, Masayoshi Shimo, and Kison Han for their assistance in experiments. This work was partly supported by a Grant-in-Aid (09640670) from the Ministry of Education, Science, Sports, and Culture of Japan. The Shimadzu GCMS-QP5050A gas chromatograph/mass spectrometer was purchased with the 1999 Fund for Special Research Projects at Tokyo Metropolitan University.

Supporting Information Available: X-ray crystallographic files in CIF format for complexes **4**, **5**, and **8**, optimized total energies of the chloro(dimethyl sulfoxide)ruthenium complexes with TPA derivatives calculated by MM (CAChe) and DFT (Table S1), Cartesian coordinates of the structures optimized by MM or DFT calculations with B3LYP/LANL2DZ or B3LYP/3-21G**, respectively (Tables S2−S4), catalytic oxidation of adamantane by ruthenium complexes with MCPBA in various solvents (Table S5), absorption changes monitored at 420 nm in the thermal isomerization of **2** (Figure S1), Eyring's plot for the thermal isomerization of **2** (Figure S2), and ^1H NMR spectra (270 MHz, Me_2SO-d_6) of (a) complex **3**, *trans*(Cl,N_{amino})-[RuCl(TPA)(Me_2SO)]$^+$, (b) complex **2**, *cis*(Cl,N_{amino})-[RuCl(TPA)(Me_2SO)]$^+$, before heating, and (c) complex **2** after heating for 6 h at 100 °C (Figure S3). This material is available free of charge via the Internet at http://pubs.acs.org.

IC060722C

(57) Ingold, K. U.; MacFaul, P. A. In *Biomimetic Oxidations Catalyzed by Transition Metal Complexes*; Meunier, B., Ed.; Imperial College Press: London, 2000; Chapter 2.